Addis Ababa University

Addis Ababa Institute of Technology

School of Electrical and Computer Engineering

(Control Engineering)

FUZZY LOGIC CONTROLLER OF DC-AC MICRO-GRID BIDIRECTIONAL INTERFACING THREE PHASE VOLTAGE SOURCE CONVERTER.

A thesis Submitted to the Addis Ababa Institute of Technology, School of Graduate Studies, Addis Ababa University in the Partial Fulfillment of the Requirement for the Degree of Master of Science in Control engineering.

By

Eual Sileshi Daka

Advisor:Dr.Mengesha Mamo

ADDIS ABABA, ETHIOPIA

October 2021

Addis Ababa University

Addis Ababa Institute of Technology

School of Electrical and Computer Engineering

(Control Engineering)

FUZZY LOGIC CONTROLLER OF DC-AC MICRO-GRID BIDIRECTIONAL INTERFACING THREE PHASE VOLTAGE SOURCE CONVERTER.

By: Eual Sileshi Daka

APPROVED BY BOARD OF EXAMINERS

	_____	_____
Chairman, Department of Graduate Committee	Signature	Date
Dr.Mengesha Mamo:	_____	_____
Advisor	Signature	Date
Nebiyu T.	_____	_____
Internal examiner	Signature	Date
Dr.Chala Merga	_____	_____
External Examiner	Signature	Date

Declaration

I, the undersigned declare that this Thesis is my original work, and has not been presented for a degree in this or any other university, and all sources of materials used for the thesis have been fully acknowledged.

Eual Sileshi _____

Name Signature:

Place: Addis Ababa Institute of Technology, AAiT

Addis Ababa University, AAU

Addis Ababa,

Ethiopia.

Submitted in: October, 2021

This thesis has been submitted with my approval as a university advisor

DR. Mengesha Mamo _____

Name Signature:

Acknowledgement

I would like to express my gratitude to all those who gave me the possibility to complete this thesis. I am deeply indebted to my advisor Dr.Mengesha Mamo from the Addis Ababa University; power electronics and Electrical drives Department for stimulating suggestions and encouragement that helped me in all the time of research and writing of this thesis. My family and friends supported me in my research work; I want to thank them for all their help, support, interest and valuable hints.

Abstract

Renewable energy formed distributed generators (DGs) play a highest role in electricity requisite and reduced in the global warming. Distributed generation formed on wind, solar energy, biomass, mini-hydro along with use of fuel cells and micro turbines are becoming a more important energy source option in the future generation system. Advantages like environmental advocate, expandability and flexibility has made scattered generation, powered by various renewable and non- renewable micro sources, an attractive option for design modern electrical grids. The micro-grid concept initiates the reduction of numerous reverse conversions in an individual AC or DC micro-grid and also solution of connections for variable renewable AC-DC sources and loads of power systems. To the end customer the micro-grid be designed to addressed their special requirements; such as, improvement of local reliability, reduction of feeder losses, local voltages support, increased efficiency through use correction of voltage sag or uninterruptible power supply. This thesis provides a study of the control scheme for interconnection of interlinking converter(IC) between a DC bus bar and an AC bus bar. Here photovoltaic system and, wind turbine generator are used for the development of micro-grid. The models are designed for the converters to affirm stable system under various loads and resource conditions and also the control methods are studied. The maximum power point tracking (MPPT) algorithm is used to harness maximum power from DC sources and to coordinate the power exchange between DC and AC bus bar. The control of interlinking voltage source converter model in dq reference which is the cross-coupling between the two orthogonal dq axes. Using voltage sensor, the Fuzzy logic controller identifies the power load demand based on the design range. A possible control scheme is studied and simulated in MATLAB Simulink. The system behavior is analyzed by subjecting it to different changes in parameters, DC load and AC load conditions.

Key words: Distribution Generations (DGs), Voltage source inverter (VSI), Fuzzy logic controller (FLC),SIMULINK® simpower system™/MATLAB®.

Table of Contents

List of Table

List of Figures

List of Symbol

$i_{d\ ref}$ =Active current reference (A)

$i_{q\ ref}$ = Reactive current reference (A)

Q_{ref} = Reactive power (W)

$V_{dc\ ref}$ =Volt of direct current reference

V_{out} = Output voltage (V)

m_i = Amplitude of modulation index

V_r = High frequency triangular carrier wave

V_c =Sinusoidal control signal

m_f =frequency of modulation index

f_r =frequency of modulating (Hz)

f_1 = frequency of carrier (Hz)

f_s = Switching frequency (Hz)

D = Duty cycle

θ = Phase angle

C = Capacitor (F)

R_f = Resistor of filter (Ω)

L_f = Inductor of filter (H)

W_g = angular frequency of AC bus.

W_n = Natural frequency of the system

ξ = damping factor

T_s = Settling time(s)

P_{air} =power contained in the wind

ρ = the air density

A = the swept area

V_{∞} =t the wind velocity without rotor reference

C_p = power coefficient

C_{PV} = capacitor across the solar cell

C_d = Capacitor across the DC-link

S= Irradiation

List of Abbreviations

FLC	Fuzzy logic controller
AC	Alternating current
DC	Direct current
dqo	Direct-quadrature zero
VSC	Voltage source converter
IGBT	Insulated gate bipolar transistor
PWM	Pulse width modulation
SPWM	Sinusoidal pulse width modulation
V_d	Direct active voltage
I_d	Direct active current
V_q	Quadrature reactive voltage
I_q	Quadrature reactive current
DG	Distribution generation
PFC	Power factor control
LED	Light emitting diode
MG	Micro grid.
IC	Interface converter
I_{pv}	Current of photovoltaic (A)
V_{PV}	Voltage of photovoltaic (volt)
VSI	Voltage source inverter
MPPT	Maximum power point tracking

CHAPTER-ONE

1. INTRODUCTION TO MICROGRID

1.1. Background

As electric distribution technology steps into the next century, many trends are becoming noticeable that will change the requirements of energy delivery. These modifications are being driven from both the demand side where higher energy availability and efficiency are desired from the supply side where the integration of distributed generation unit. In order to solve this problem integrate distributed generation conception, micro grid as a new idea has then been proposed to well manage the local DG units and loads. Generally micro-grid concept defined as a local electric power distribution system with diverse distributed generation units, energy depository systems, and loads, which can operate as a part of the distribution system, in both grid-connected and islanded modes [1], [2]. Over the years in Ethiopian, many works related to micro-grids have been developed aiming at improving the operation of modern electrical systems with high penetration of distributed generation [3].

1.2. Overview of the thesis

Based on the outputs of the participating DG units and loads, micro grids can be classified into AC, DC and hybrid DC/AC type through three phase inter-linking converter in figure 1.1.The AC micro grid, the DC produce a sources such as PV, converted to AC with the use of DC/AC converters based on the load demand, while AC produces a sources are directly joined using power electronic interfaces. With high perception of DG units,[4–5], has more capacity and control flexibilities to be attached to the conventional AC power systems. However, some new energy source in the micro grid, such as photovoltaic (PV) panel is DC source in nature. Whereas, DC micro-grids AC producing sources are converted to DC using DC-AC converters based on the load demand. For the present, many DC loads, e.g. LED lighting and computers etc., are highly growing at the end users,

which need the power factor correctors (PFCs) to change the standard AC voltage to a desired DC voltage. Therefore in order to fix power needs of at the customer both DC and AC micro-grid to merge through a bidirectional DC-AC converter establishing in which DC or AC source and load can flexibility integrated and power can flow smoothly flow between the two micro-grid.

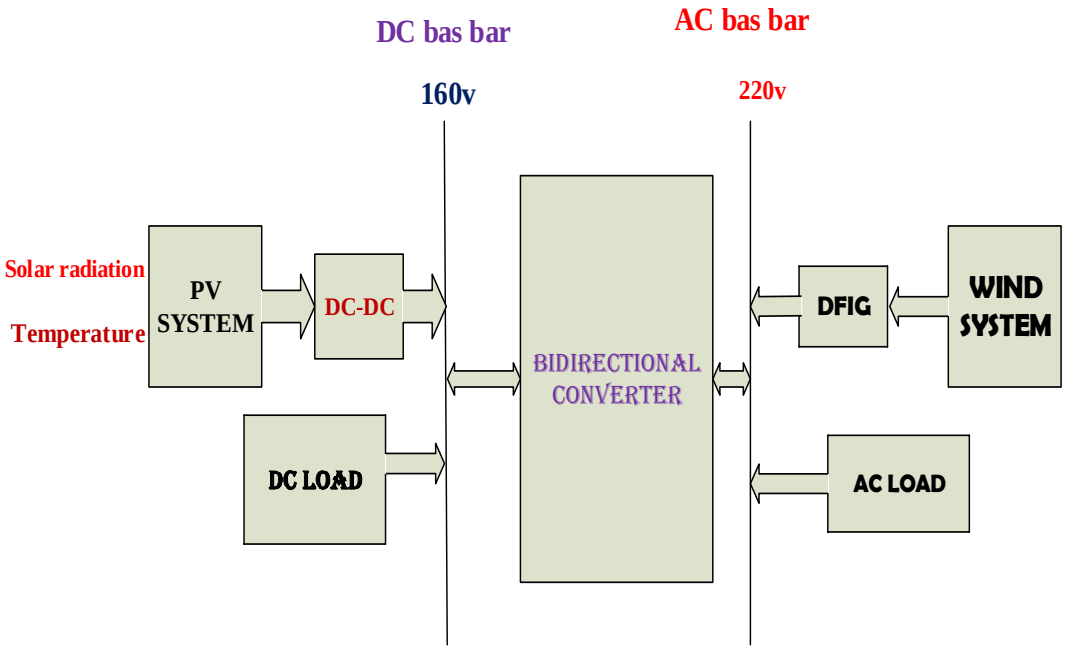

Figure 1. 1block diagram of DC-AC micro-grid interlinking converter control.

Inbuilt, established a DC power is supply to connect the DC sources and DC loads instantly using high efficient DC-DC boost converters could reduce the unessential power conversion circuit and make simpler the control complexity.So,the DC micro-grid can show its significant features with high efficiency and low power conversion cost. The DC micro grid has been proposed in [6–9] to combine various distributed generators.

In study of , many DC micro-grid pilot projects, such as low voltage DC micro grids at the Italian Research Center on Energetic Systems and the Lawrence Berkeley National Laboratory, have been well- established and tested with 10% energy savings for their data center compared to a very efficient AC base line case. Compared with AC micro grid, DC micro grid has other advantages of less energy conversion links, lower line losses and higher system efficiency. In addition, the DC micro grid does not need to track the phase and frequency of AC voltage unlike the traditional grid tied inverters, which greatly influence the controllability and the reliability of AC micro grid. Therefore, DC micro grid is extra suitable for the integration of distributed generations of renewable energy sources.

However, for all-inclusive micro grid, where the various sources as complementary should be unified to solve the environmental impact and reduce the interruption maintenance time, a pure DC micro-grid would be deemed inappropriate. Therefore, DC-AC micro grid should be assumed to fully demonstrate the advantages of AC and DC distribution networks in view of easier renewable energy integration, higher power conversion efficiency, less energy storage capacity, and higher reliability. In general, the merit of cross DC-AC micro grid are the reduces of unnecessary AC-DC or AC-DC-AC power transformation circuits installed in the power supplies, meaning the significant reduction of power conversion losses, the reduction of embedded PFCs for powering DC loads in the traditional AC grid, meaning the notable cost and loss reduction of power electronics equipment at end customer, the upgraded power quality in AC micro- grid; since the DC loads will not directly generate harmonics pollutions and the three phase interlinking converters with full controllability can significantly increase the power quality; The upgraded unsymmetrical current control capability has been negative and zero sequence current issue caused by the unbalanced loads in AC grid can be controlled by the DC grid can be summarized as follows [10, 11]:

In this architecture, this thesis reviewed the solar plant connect through DC/DC boost converter and DC load are connected DC bus bar.

whereas wind source and AC load are interconnected to AC bus bar .The main components of such an interconnected the DC bus bar and AC bus bar are three phase Voltage Source Converter (VSC), the control mechanism and the filter. Then using DC-AC micro-grid, the bidirectional interlinking converter is voltage source converter (VSC) which is implemented in dq reference frame to control the two ways of power flow based on the DC and AC load. This interlinking voltage source converter with one inner loop current PI controller and one output voltage PI controller. Both controllers are to increase the power efficiency in island mode and grid connected mode. This thesis extends the FLC identify the load demand on both side DC-AC hybrid micro-grids using voltage sensor. Database contains of input and output membership functions and supply information for appropriate fuzzification step and defuzzification operations. The rule-base formes of a set of linguistic rules link with the fuzzified input variables to the desired control actions. Fuzzification converts a crisp input signals, error (e), and change in error (ce) towards fuzzified signals that has been identified by level of memberships in the fuzzy sets. The inference method's uses the collection of linguistic rules to convert the input conditions to fuzzified output. Lastly, the defuzzification with changes in the fuzzified outputs to crisp control signals using with the output membership function, which has the system take stepes as the changes in the control input (u).The defuzzification method's used here is built upon centroid method. The fuzzy logic controller (FLC) was used to pick out the AC load voltage and DC load using voltage sensor. The advantages of this type of control are to increase the power efficiency of the system, to minimize conversion loss and it permit the system operative to control independently of the active (d-axis) components and reactive (q-axis) components of the currents, voltage and power. Finally,the feasibility and the suggested control strategy are verified by simulation results on MATLAB/Simulink.

1.3. Statement of the problem

Agreement to EEPCO data, current data with only 17% of households connected and 41% of the population is calculated to have access to electricity and the per capital energy consumption is 100kWh, which is the lowest in the sub-Sahara average, that is 510kWh. [www.mowe.gov.et]. Maximum of the non-electrified regions are found especially in rural part of the countries. Those regions can be electrified furthermore by extending the micro-grids of the in existence power systems or by constructing standalone power systems. In general, micro grid electrification concept for remote place is nowadays becoming attractive and another option for remote villages 'for specific home, and to give the opportunity which are detached from the central grid. There is a large possible for utilizing renewable energy sources, for example solar energy, wind energy, to provide a quality power. The Ethiopia Government is now aware the national utility alone through Continuous grid extension cannot speed up rural access to electricity. In order to solve this causes this thesis will proposed Scaling up renewable energy integrating in DC-AC micro-grid interfacing converter control to increase the power efficiency of the system and for the purpose of reduces the reversible conversions smooth power variation between sources and maintain stable operation in the system. Interlinking converter to facilitate the power flow of in between DC micro grid and AC micro grid.

1.4 .OBJECTIVES OF THE THESIS

1.4.1. General objective

The main objective of this thesis is to study the feasibility of fuzzy logic controller DC-AC micro-grid bidirectional interfacing three phase voltage source converter.

1.4.2. Specific objective.

- To connect renewable energy of PV modules to DC bus bar and Wind module to connect AC bus bar to increase the system power efficiency.
- Bidirectional interlinking converters between AC and DC sub-grid to reduce repeated power conversion losses.
- Control of the converter two way power flow in abc to dq reference frame.
- Sensing generated power and load on both sides using matlab Simulink.

1.5. Significant of the study

The scope of this inquiry is to assess the technical and economically feasibility of DC-AC Micro grid converter control energy system to supply the rural community detached village from the existing national grid in Ethiopia. The study will investigate different renewable energy option to satisfy the energy demand and to increase the power efficiency of the village. This study should collect the load demand, analyzed relevant data, information to examine and select the most suitable systems configuration, recommend necessary action, necessary measures that configure a system to accommodate the current and near future electrical energy demand for the village.

1.6. Limitation of the study

During working research paper there is a limitation: the first limitation is lack of cooperation to get relevant data from selected area. The second limitation the rage of view of the study is very complex control strategy when it goes from individual AC sub micro-grid and DC sub micro-grid into hybrid DC-AC micro-grid. The third limitation is unable to get the research money at the essential time.

1.7. Outline of the thesis

The Thesis is arranged into six chapters.

Chapter One: Presents the Introduction, overview of the thesis, Statement of the problem, Objectives of the thesis and Method leading towards the completion of the thesis.

Chapter Two: Basic theory and literature review on DC-AC micro-grid.

Chapter Three: Deals with the classification of operation in a hybrid DC/AC micro-grid. Modeling of DC micro grid component, modeling of AC micro-grid, configuration and control mechanism of hybrid DC/AC micro-grid, power flow stage and control of three phase voltage source converter in dq reference frame and load demand identify using fuzzy logic controller.

Chapter four: Discussion about the simulation results of the hybrid components, the power flow in dq reference frame and Fuzzy logic controller in matlab/Simulink 2019a.

Chapter Five: Explain about conclusions, recommendation and future work.

CHAPTER-TWO

2. BASIC THOREY AND LITERATURE REVIEW

Different researches have been carrying on DC-AC micro grid power generation all over the world and in Ethiopia. Different scholars used different Technology alternative and approaches to evaluate the various configurations of renewable energy resources, such as solar energy, wind energy, small hydropower and their hybrid configurations as follow. Berihun G. (2013) presented reported of rural area in Ethiopia entitled "Modeling and Simulating of a Micro Hydro-Wind cross-over of power generation system for rural area of Ethiopia" by using HOMER software. He discussed two ways, Wind/Micro hydro hybrid and Standalone large hydro system by comparing the cost of energy to identify cost competitive for the remote village compared to extending the existing grid to the area. According to Him, Wind/Micro hydro hybrid system is $0.112/kWh. Moreover, COE of standalone Micro-hydro system is $0.035/kWh. He concluded micro hydro system is the most economical and can only satisfy the energy demand of the village and technically feasible option [46]. Still his hybrid configuration is not consider the load demand, only one direction power flow and is not consider the power efficiency only considered the cost.

Gelma Boyena [47] developed Design of a Photovoltaic/ Wind cross-over Power generation system for Ethiopian remote area. The author aim had to design and model a stand-alone PV-Wind cross-over power supply system for Balley and Surrounding areas of 100 households and community services. The author discussed that for those community isolate from the central grid, life style of the target community could be improved by promoting a cost effective PV-wind hybrid system. He simulates the suggested hybrid system and the result obtained affected by the renewable energy access. The author pointed out that this tariff is higher than the current tariff of the country. However, from Social point of view and improvement of the life of the people not connected from the central grid the cost is not such significant.

For the off grid system single technologies such as solar photovoltaic system and wind turbine are unable work reliable and reduce the power efficiency due to their variability of resources and high conversion loss.

A research conducted by Leak. E Woldemaria entitled" Genset Solar-Wind hybrid power system of off-grid power generation for rural application. The hybrid system comprises of generators set PV–array and wind turbine with storage and power electronics device presented in his paper. His study intended to promote an efficient and cost competitive system configuration of cross-over power system to improve the life of the rural community not yet connected to the central grid. According to my suggestion he could not consider power balance between EG_S in the grid, one of the main drawbacks of distributed generation systems based on renewable sources is their controllability of power flow. If the systems model is not correctly controlled to the main grid, it can lead to the instability, or even failure of the system. Moreover, the degrees for interconnecting those systems to the point network are stressing more on the capability of to run over short grid disturbances [48]. Therefore, the control strategies applied to distributed systems become of high interest limited in seasonal and single technology in EG_S.

Getachew, B and Palm [49] studied the alternative of contribute electricity from solar-wind cross-over system to a remotely located community of 200 families isolated from the national grid in Ethiopia through HOMER software. The results were compared from the list of feasible renewable power sources sorted based on net present cot and found that hybrid solar and wind system is only the promising technology for power generation to these communities. In this scholar's did not consider the load and high reversible conversion loss. All most all of the above scholar's paper shows the hybrid system either only PV/wind excluding hydro, Dessile generator or PV/Wind/Hydro Exclude wind turbine and did not consider the power load demand in both side . But in this thesis studded to consider combine PV, to the DC system through DC/DC boost circuit.

AC system structure of micro-grid interface is similar to DC system structure, wind turbine an AC source and load to AC bus bar. The cooperation control algorithms are suggested to control the power in flow between DC and AC grids and to maintain both AC and DC voltages. Uncertainty and recurring feature of wind rotor speed, solar irradiation level, ambient temperature and AC load and DC load capacities are also meditated in system design control and operation. The simulation outcome shows that system is exist under different load and supply conditions. Moreover, the hybrid micro-grid has higher performance than individual AC or DC micro grid for reduces of multiple DC-AC-DC transformation. The DC-AC bus bar bidirectional interlinking converter plays an advantage role in this kind of structure which can coordinate the power flow and control in the operation state of DC-AC micro grid interfacing system and it increase power efficiency. From the controlling point of view, this thesis reviews the most important part of a hybrid DC-AC micro grid is the interlinking converter controller which links the DC bus with the AC bus. The interlinking converter controller consists of two inner loop controllers for both islanded and grid connected operation of the micro grid. These inner control loops are power controller, voltage controller and current controller. Three phase Voltage source converters (VSCs) are among the main building blocks of power generation systems and they are commonly used for interfacing renewable energy sources.

VSCs have many advantages including current and voltage in regulation, active power filtering and power factor control. Voltage source converters require exact control to achieve the desired objectives in presence of the system nonlinearities and the unknown disturbances. Several works has been addressed voltage source converters output voltage and current control in the last century. The main concept is to outline a cascade control system design, where the inner loop is done for current control and the outer loop is done for voltage control. In inverter-based distributed generators control, synchronous (direct-quadrature d-q) reference frame is used as the manipulated variables. The VSC control system uses PI controllers for both current and voltage control.

In this thesis a fully separated interlinking control system is designed for both current and voltage control of voltage source converters with LC output filter apply in the d-q reference frame. Low pass filters after converting the abc quantities into the dq quantities. Another option is to pre-filter the quantities after measuring them at the PCC and then do the conversion to the dq reference frame. For proper power flow in between DC and AC sub grid fuzzy logic controller scheme implemented. In fuzzy logic control, main control method is driven by a set of linguistic rules which are determined by the system. Since numerical symbol are changed in to linguistic variables, modeling of mathematical system is not needed. In the first step, the degree of crisp inputs is based on each fuzzy set is decided. These fuzzified inputs are the DC load and AC load then fed to the inference mechanism in order to evaluate the fuzzy rules stored in the fuzzy rule base. Set of output membership functions are used for this convert based on the suitability of the application. Inference engine based on the fuzzy rules, generates the Fuzzy output values. Defuzzifier converts the fuzzy set acquired by the inference engine into a crisp value. Defuzzifier achieves output signals based on the output fuzzy sets obtained. The fuzzy logic controller (FLC) has been proposed and simulated with Matlab/Simulink for controlled the voltage source converter action. This kind of micro-grid will plane in Ethiopia in 2025G.C.

CHAPTER-THREE

3. Methodology

The concept of micro grid is studied as a collection of DC and AC loads and micro source which functions as a single controllable system that provides power to its local area and home. Govern of a hybrid micro grid first requires to control of the corresponding individual sub grids, and then coordination between the DC and AC sub micro-grids by an interlinking three phase converter control approach applied to the ICs. In this thesis focused on the methodology of the whole system and procedure to design Classification of different operation modes in a hybrid DC-AC micro-grid interfacing converter control, two way power flow, sensing generated power ,load unbalanced on both side controlled by fuzzy logic controller(FLC) and control of converter DC-AC micro-grid interfacing in dq reference frame.

3.1. Classification of operation in a hybrid DC/AC micro grid

Generally, DC-AC micro grid consists of three main parts: AC sub-micro grid, DC sub-micro grid and power electronics interface interlinking converter (IC_S) in between AC and DC buse bar. Figure 3.6. shows that a general design of hybrid DC-AC micro grid. Where the DC bua bar is connected to AC grid through three phase an inter-linking converter. The AC sub-micro grid is generally predominant in the hybrid DC-AC micro gird to provide a stable voltage. The AC distributed generator (DG), is wind turbine, and the AC loads. On the other way, DC power source such as photovoltaic panel, and DC load can be interconnected to DC sub-micro grid through simple DC-DC boost converter. The main focused of this thesis is to control of the power flow on both side by interlinking converter in between AC bus and DC bus bar in dq reference frame based on the load demand. The main reason to transform the three-phase instantaneous currents and voltages forward the synchronously rotating reference dqo frame is to make figuring much easier. Secondly, it permits the system operation to separately control the active (d-axis) and reactive (q-axis) components of the current, voltage and power.

3.1.1. DC micro-grid

In DC micro grids the main components of are PV array, DC-DC boost converter, load and the maximum power point tracking (MPPT) control algorithm. DC-DC boost converters for PV applications are the ability to supply a high voltage output from a low voltage input. MPPT methods had used for more extracting maximum available power from PV model under a particular condition of environmental by controlling of based on the duty ratio DC-DC converter. Based on maximum power flow theorem, by varying the duty cycle, the load resistance was seen by the source is changed and matched with the internal resistance of PV model at maximum power point (MPP) so as to flow the maximum power. Under sudden varies in solar irradiance and temperature, for the selection of MPPT ways of algorithm's sampling time (TS_MPPT) is highly dependent on two main components of the converter circuit namely; inductor and capacitor. In DC micro-grid DC voltage is the only control variable which can control the active power among the converters. The parameter like reactive power and frequency are not relevant to the DC sub-grid, and do not participate in power sharing scheme.

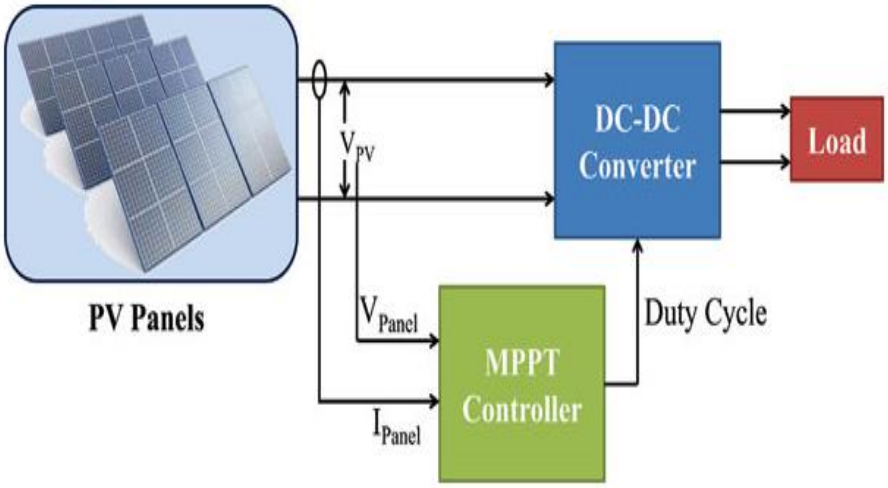

Figure 3. 1MPPT PV systems with load resistor in DC micro-grid.

3.1.1.2. Photovoltaic system

A photovoltaic system makes use of more solar panels to convert solar energy to electricity. It has different components which are the photovoltaic modules, mechanical, electrical connections, mountings and ways of regulating and/or remodel of the electrical output.

3.1.1.3. Modeling of PV panel

The photovoltaic model system can produce direct current electricity without environmental strike when it is exposed to sunlight. The main model block of PV arrays is the solar cell, which is mainly a p-n junction that directly changed to the light energy into electricity. The output attribute of photovoltaic module based on the cell temperature, solar irradiation, and output voltage of the module. The figure.3.2. Shows the overall circuit of a PV array.

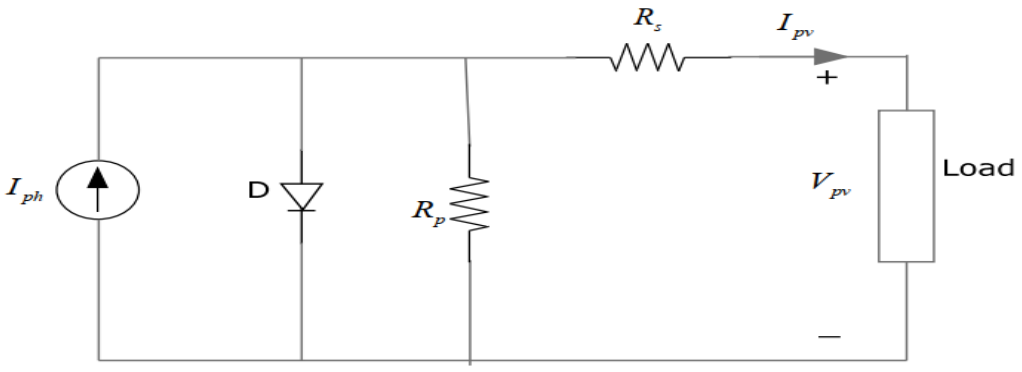

Figure 3. 2Equivalent circuit of a solar cell

Usually the overall circuit of a general solar cell model consists of a photocurrent, a diode, a parallel resistor which expresses a leakage current, and a series resistor which describes an internal resistance to the current flow. The voltage current characteristic equation of a solar cell is given as:

$$I = I_{ph} - (I_s)^{((V+I*R_s)/(N*Vt))-1} - I_{s2}^{\left(\frac{V+I*R_s}{N_2*Vt}\right)-1)-(V+I*R_s)/R_p} \text{ ----------(3.1)}$$

Where Is2 and Is are the diode saturation of current ,V_t is the thermal voltage, N2 and N are the quality factors of (diode emission coefficients) and I_{ph} is the solar produced current. The PV current mainly based on the cell's working temperature and solar irradiation, which has the short-circuit current I_{sc} and short-circuit voltage V_{oc} are the two basic important parameters used which depict the cell electrical performance.

The quality factor varies the solar cell and typically has a value in the range of 1 to 2.The input I_r is the radiation falling on the cell. The solar-generated current I_{ph} is given by:

$$I_{ph} = I_r * (I_{pho}/I_{ro}) \text{ ----------(3.2)}$$

Where I_{pho} is the measured solar-generated current for irradiance $I_{ro.}$

Then, the maximum power can be gained as:

$$P_{max} = V_{max} * I_{max} = V_{oc}I_{sc} \text{ ----------(3.3)}$$

Table 3. 1Specification of solar PV model.

No	Parameter	unit	Value
1.	Short circuit current (I_{sc})	Ampere	8A
2.	Open circuit voltage(V_{oc})	Volt	12v
3.	Output power(Pout)	watt	92w
4.	Solar radiation(S)	w/m^2	(0-1000)w/m^2
5.	Temperature(T_c)	degC	(0-50)degC
6.	Energy exponent for I_s		3
7.	Reference temperature(T_{ref})	degC	50degC

3.1.1.4. Maximum power point tracking

As a system of maximum power points tracker (MPPT) functions the photovoltaic (PV) models is the way that allows the PV models to produce all the power they are efficient of. It has not a mechanical tracking model which moves actually the model to make them point more directly at the sun. Since maximum power point tracker (MPPT) is a fully electronic model algorithm, it differs the module's set values, so that, the models instant able to carry maximum power. The PV system outputs are based on the temperature, irradiation, and the load behavior MPPT cannot carry out the output voltage perfectly. For this condition MPPT is needed to be implemented in the PV system to maximize the PV array output voltage. Necessary of maximum power point tracking shown in the figure.3.3.

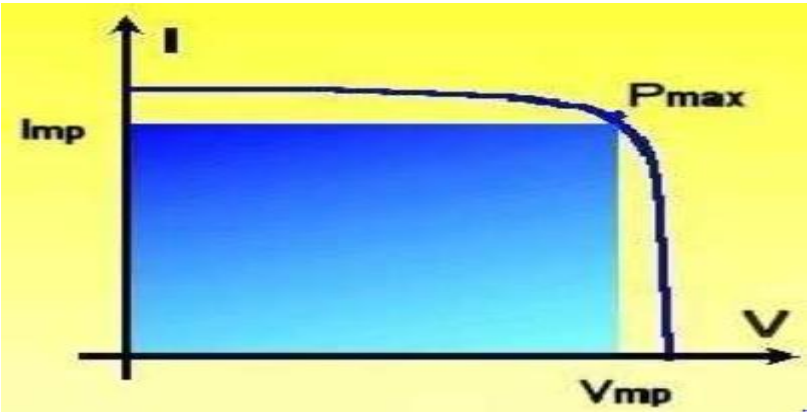

Figure 3. 3MMPT characteristic

In the power versus voltage curve of a PV module there exists a single maxima of power, i.e. there exists a peak power corresponding to a particular voltage and current. The efficiency of the solar PV module is low about 14%. Since the module efficiency is low it is advisable to operate the module at the peak power point so, the maximum power can be delivered to the load under varying temperature and irradiation varies conditions. This maximized power helps to improve the use of the PV module.

A maximum power points tracker (MPPT) extracts high power from the PV module and transfers this power to the load. As an interfacing device DC-DC boost converter transfers this high power from the solar photovoltaic module to the load. By varying the duty cycle, the load impedance is changed and matched at the point of the peak power with the source so as to transfer the maximum power.

3.1.1.5. Algorithms for tracking of maximum power point

There are different algorithms which help to track the peak power point of the solar PV module automatically from those algorithms this thesis is used Perturb and observe method.

3.1.1.6. Perturb and observance method

The algorithm is the flowchart of continuously increments or decrements the reference voltage based on the values of the previous power sample.

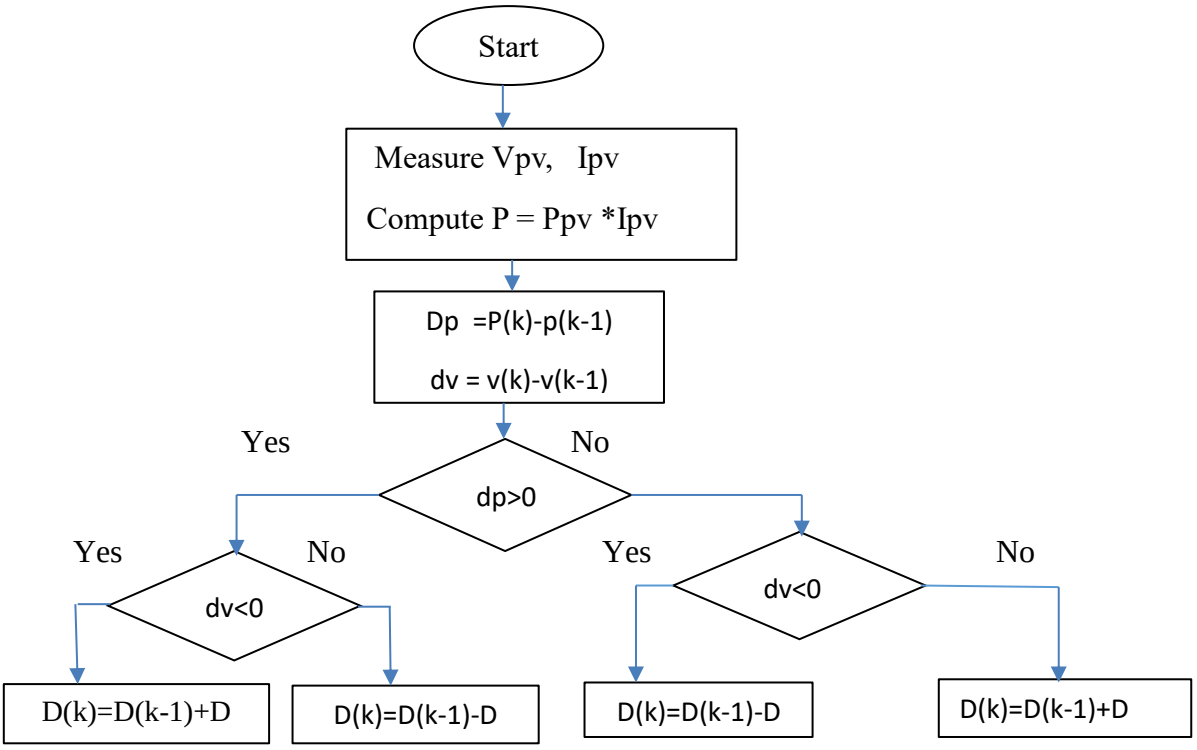

Figure 3. 4 Flowchart Perturbs and observe algorithm

3.2. AC micro-grid

The renewable energy wind turbine AC source can connect to the AC sub-micro grid through the interfacing converters. In AC-micro grid, voltage and frequency are the control variable which can control among the converter. In this thesis wind turbine is model it's power output in matlab Simulink.

3.2.1. Wind turbines system design

In the use of power of the wind, wind turbines produce electricity to drive an electrical generator. Usually wind passes over the blades, generating lift and exerting a turning force. Inside the nacelle the rotating blades turn a shaft then goes into a gearbox. The gearbox helps in increasing the rotational speed for the working of the generator and utilizes magnetic fields to convert the rotational energy into AC electrical energy. Then the output of electrical power pass to connected to AC bus, which changes the electricity for the appropriate voltage of the power collection system. The wind turbine pull out kinetic energy that of swept area of the blades. The power consists in the wind is given as the kinetic energy for transferring air mass per unit time. The equation for the power carried in the wind can then be written as:

$$P_{air} = \frac{1}{2}(\text{air mass per unit time})(V_{\infty})^2 \text{----------(3.4)}$$

$$P_{air} = \frac{1}{2}(\rho A V_{\infty})(V_{\infty})^2 \text{----------(3.5)}$$

$$P_{air} = \frac{1}{2}(\rho A V_{\infty})(V_{\infty})^3 \text{----------(3.6)}$$

Although Equation. (3.6) describes the availability of power in the wind; power transferred to the wind turbine rotor is reduced by the power coefficient C_p.

$$C_p = \frac{P_{\text{wind turbine}}}{P_{air}} \text{----------(3.7)}$$

A maximum value of C is explained by the Betz limit, which states that a turbine can never extract more than 59.3% of the power from an air stream.

The wind turbine rotors have maximum C_p values in the range 25-45%.

$$P_{\text{wind turbine}} = C_p \, xP_{air} \text{----------(3.8)}$$

Table 3. 2Parameters of wind turbine

No	Parameter	unit	Value
1.	Nominal mechanical output power	watt	1.5kW
2.	Based power of electric generator	VA	1.6kW
3.	Base wind speed	m/s	12
4.	Maximum power at base wind speed(pu nominal mechanical power)		0.73
5.	Base rotational speed(pu of base generator speed)		1.2
6.	Pitch angle	Degree	3
7.	External wind speed	m/s	400
8.	Rating power	kw	248kw

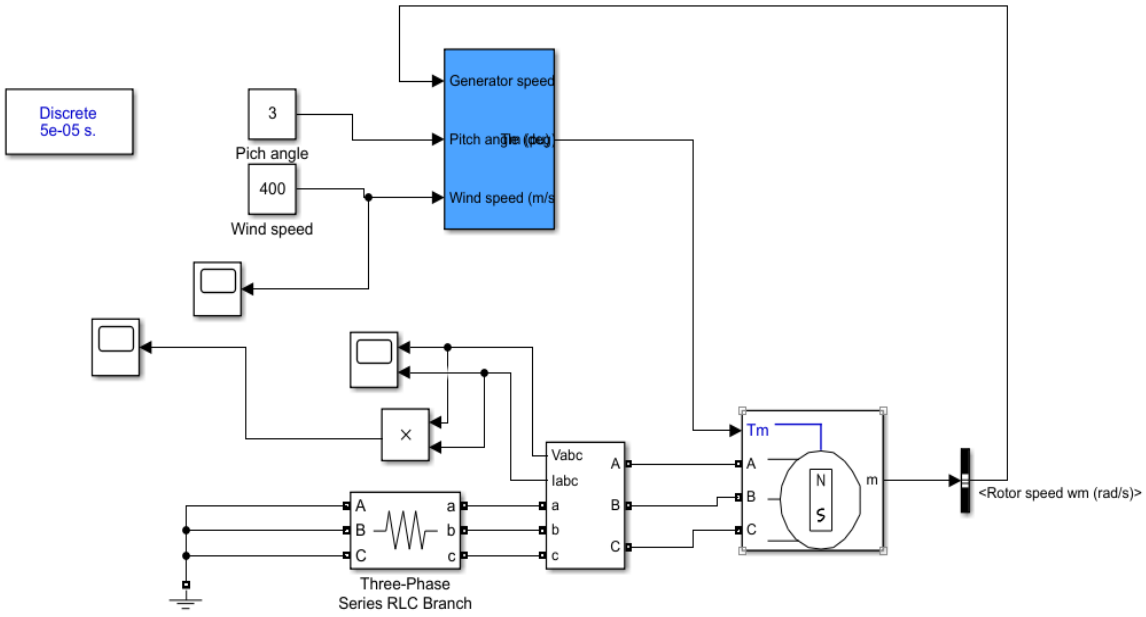

Figure 3. 5Matlab modeling of wind turbine

3.3. Configuration of hybrid DC/AC micro grid

Figure 3.6.shows a simple flexible structure of hybrid DC-AC micro-grid which is formed by one AC micro-grid and one DC micro-grid connected together through an interfacing converter (IC). The AC distributed generator (DG), is AC source wind turbine, and the AC loads. On the other hand, DC power source such as photovoltaic panel, and DC load can be interconnected to DC sub-micro grid through simple DC-DC boost converter. The sub grids in the hybrid system are handled their local loads. The interlinking converter provides bi-directional power flow between the two sub grids depending on the load demand supply suppression in the individual sub grids. The power split in both sub-bus bars would highly dependent on the control methods of interlinking converter in dq reference frame.

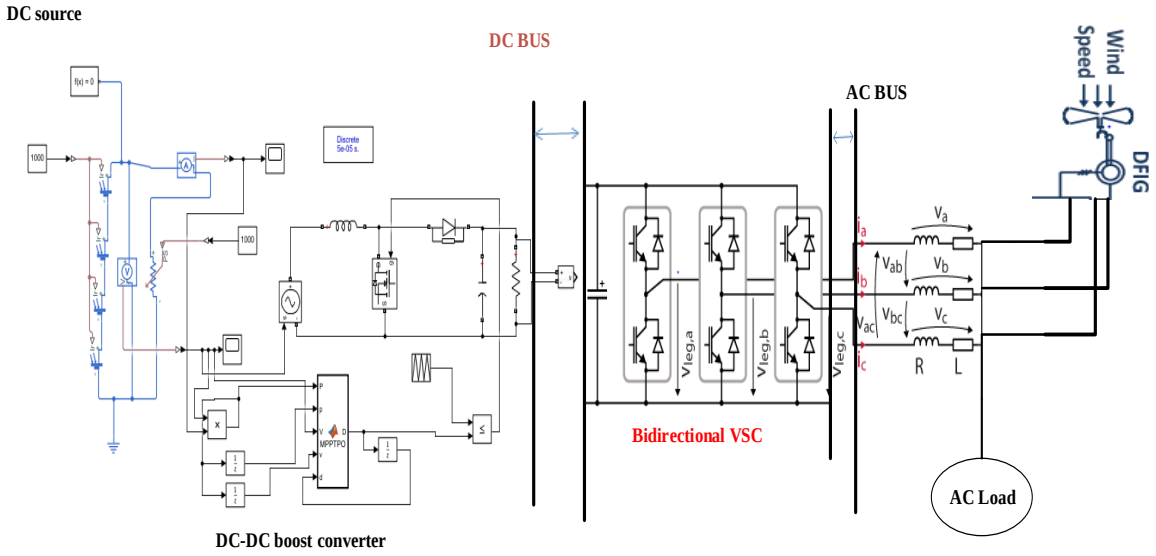

Figure 3. 6 Configuration of DC-AC micro grid

The interlinking three phase converter whose responsibility was to link DC and AC sub micro-grids and to implement the power flow in between AC bas bar and DC bas bar simply to use three phase voltage source converters (VSC**).**

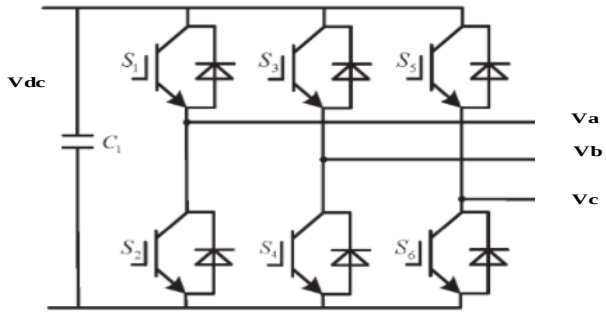

Figure 3. 7Configuration of three-phase AC/DC converter

Consists of six IGBTs, which form a three-phase AC to DC converter. Figure.3.7. presents a common three-phase DC-AC converter using IGBTs. Since each IGBT has a reverse parallel diode, the current has the capability to flow back and forth in between DC and AC side. Therefore, the VSC could either operate like rectifier or an inverter without any topology change.

3.3.1. Topology of IGBT

IGBT is a fusion between a BJT and MOSFET a three-terminal of semiconductor switching device that have input side shows a MOSFET with a Gate terminals and the output side shows a BJT of Collector and Emitter. The conduction terminals of Collector and the Emitter are the gate that which control terminal with which has been switching operation is under controlled. Although it's used for high switching purpose with high efficiency in numerous types of electronic devices and high current application. These devices are used for amplifies of switching processing complex wave patters with pulses width modulation (PWM)..The figure.3.8.shown below IGBTs with voltage rating likely to 6.5 kV are available [45], and for high-voltage applications, need to be interconnected in parallel the typical current rating is around 1.2–1.5 kA . A transistor symbol is depicted in Figure.3.8.a, with terminal names: collector, emitter, and gate.

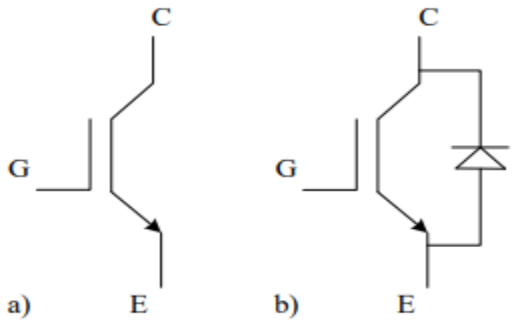

Figure 3. 8 a) IGBT symbol; b) IGBT with antiparallel diode

Fig.3.9.Shows the current-voltage characteristic of an IGBT. When the voltage between the collector and the emitter (V_{CE}) is positive, and a gate is short-circuited with the emitter, an IGBT is forward-blocked. To switch the valve from the blocking to the conduction state, it is necessary to bring the gate terminal voltage (V_{GE}) to a sufficient level. When the voltage between the collector and the emitter is negative, the device is in reverse-blocked state. However, reverse blocking is not necessary for typical high-voltage configurations since an antiparallel diode is added to the transistor (symbol in Fig. 3.8.b). Antiparallel diodes enable current transfer in opposite direction and protect transistors from reverse over voltage. The characteristic curves that correspond to the collector current is shown in relation to the voltage. In high voltage applications, an IGBT is always operated in the saturated region of the curve.

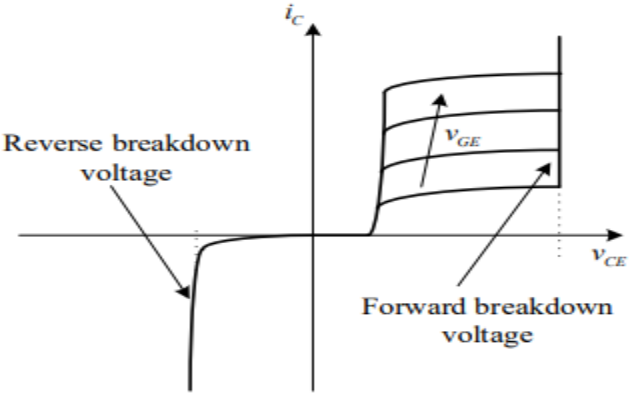

Figure 3. 9IGBT current-voltage characteristic

Inverters in MG based on their functions can be dividing into three groups according to their function: grid following or feeding), grid forming and grid supporting [41].In this thesis simply used grid following inverter.

3.4. Grid-Following: Power Export Control

The grid-following power export control methode is often used to control the output power within the voltage and frequency limits as set by the micro-grid. If the coupling converter is a voltage-sourced converter (VSC), a current-controlled strategy used for determine the reference voltage waveforms for the pulse-width modulation (PWM) of the VSC. The reference signals are also synchronized to the micro-grid frequency by tracking the voltage waveform. The control strategy can be implemented in a synchronous "dq0" frame that specifies the direct (d-axis) and (q-axis) quadrature components for converter output currents corresponding to the real and reactive output power components, respectively. Figure. 3.10.shows a block model representations of a "dq0" frame controller.

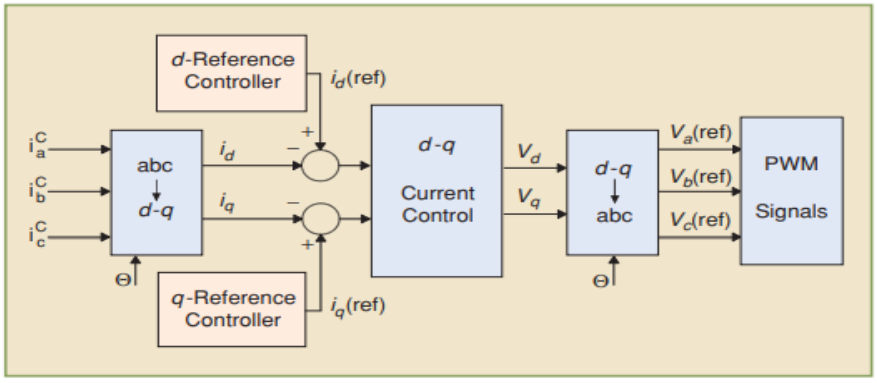

Figure 3. 10 "dq" current control of a VSC-interfaced

Figure.3.10.shows that the overall diagram of d-axis and q-axis current components of the VSC are extracted through an abc to dq0 transformation, and then compared with the corresponding reference signals that are specified by the external power or voltage control loops.

The error signals are applied to a dq current control block to set the d-q elements of the reference voltage signals V_d and V_q. Finally, through a transformation from dq0 to abc, the three-phase reference signals for the PWM signal generator are determined. Both the internal and external control blocks can change based on the control modes and the type of primary source. Figure.3.11. shows a control block based on a power export strategy in which a dc coupling (PI) voltage controller and a reactive power controller replace the dq reference controllers of Figure.3.10, respectively. The input power obtained from the PV source is suppled into the DC-link, which raises the dc-link voltage.Voltage controller (PI) prevents the voltage rise up to specifying a sufficient set value of the d-axis inverter current for equalized the power in-flow and out-flow of dc-link. For reactive power PI controller of Figure.3.11 mention the reference set values for the q-component of the converter current. The Q_{ref} value is set the value to zero for case of unity power factor. Figure.3.11.also shows further details of the d-q current control, including two proportional integral (PI) controllers for the d- and q-axis current controls, the voltage feed-forward terms, and the cross-coupling elimination terms. The outputs from the current controllers, after transformation, constitute the reference voltages for the PWM signal generator.

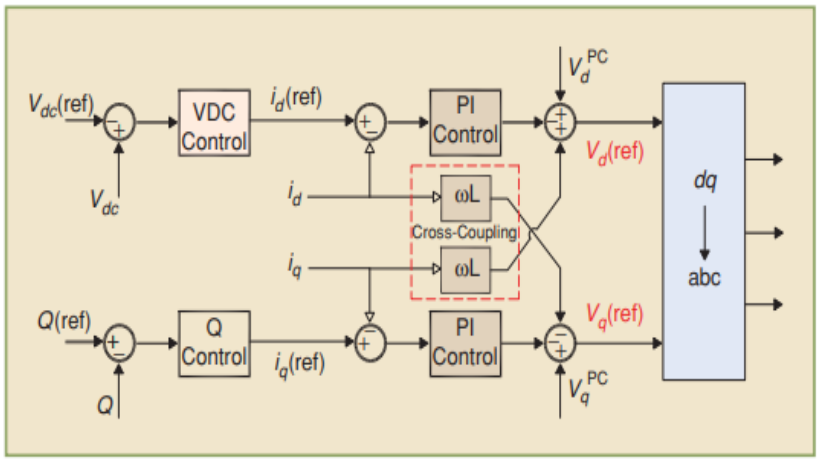

Figure 3. 11Gride-following power export control diagram

3.5. Voltage source converter

The main requirement in a power transmission system is to control of reactive and active power flow to stable the system voltage stability. This is achieved through an electronic converter and its ability of converting electrical energy from AC to DC or vice versa. Depending upon the input and output there are divides into two types of converters Voltage Source Inverter (VSC) and Current Source converter (CSC).

(a) Voltage Source Converter (VSC): In VSC, input voltage is maintained constant and the amplitude of output voltage does not depend on the load values. However, the waveform of load current as well as its magnitude depends upon the nature of the load impedance.

(b) Current Source Inverter (CSI): In this type of converter input current is constant but adjustable. The amplitude of output current from CSI is independent of load. However the magnitude of output voltage and its waveform output from CSC is dependent upon the nature of load impedance. A CSI does not require any feedback diodes whereas these are required in VSC.

3.6. Pulse width modulation technique (PWM)

In Pulses Width Modulation (PWM) technique, pulses of constant amplitude but different duty cycles are generated by modulating during the time periods. This modulation index is done by using carrier and reference signal. These two signals are fed to a comparator and the corresponding signals are generated based on the logic of the comparator. The reference wave is the desired signal output which may be a sine wave. The carrier wave, on the another way, is generally sawtooth or triangular wave having frequency significantly higher than that of the reference signal. Based on their functions the three basic pulse width modulation (PWM) techniques: Single pulse, multiple pulse and sinusoidal pulses width modulation (SPWM). In this thesis only implemented sinusoidal pulses width modulation (SPWM).

3.6.1. Sinusoidal pulse width modulation technique (SPWM)

The principle of the sinusoidal carrier-based pulse width modulation (SPWM) technique; a high-frequency triangular carrier wave Vr is compared with a sinusoidal control signal of V_c at the desired frequency. The intersection of Vc and Vr waves determines the switching instants and commutation of the modulated pulse. A transition in PWM waveform is generated at each compare match point. When sinusoidal waves have magnitude higher than of the triangular waves the PWM output is positive and when Vc is smaller than Vr, the output is negative. The inverter's switching frequency fs establishes by the frequency of triangle waveform Vc. The fundamental frequency component in the inverter voltage output can be controlled by amplitude modulation index; we define the modulation index mi as follows:

$$m_i = Vc / Vr \text{ ----------} (3.9)$$

Where Vc and Vr are the peak values of the modulating and carrier waves, respectively. The amplitude modulation index m_i is usually adjusted by varying Vc while keeping Vr fixed. The frequency modulation index is defined by:

$$m_f = fr / f_1 \text{ ----------} (3.10)$$

Where, f1 and fr are the frequencies of the modulating and carrier waves, respectively. The fundamental component V_{out1} of the output voltage has the property as depicted in equation below in a linear modulation region .In figure 3.12 shows that the modulation index and amplitude of the fundamental component of the output voltage varies linearly.

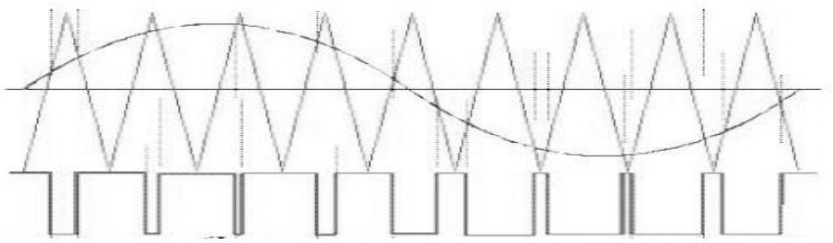

Figure 3. 12Sinusoidal PWM

The m_i value varied from zero to one; it is set as the linear control range of sinusoidal carrier PWM. Three levels pulses width modulated wave forms it's achieved in the form of sine carrier PWM. A sine carrier is achieved in comparing the three references control signals from triangular carrier waves. SPWM is applied for voltage control of three phase's inverters and the correlated gating signals are shown below in Figure 3.13.Where, triangular carriers wave related from three references sinusoidal waves (U,V,W) which are shift by 120 degrees.

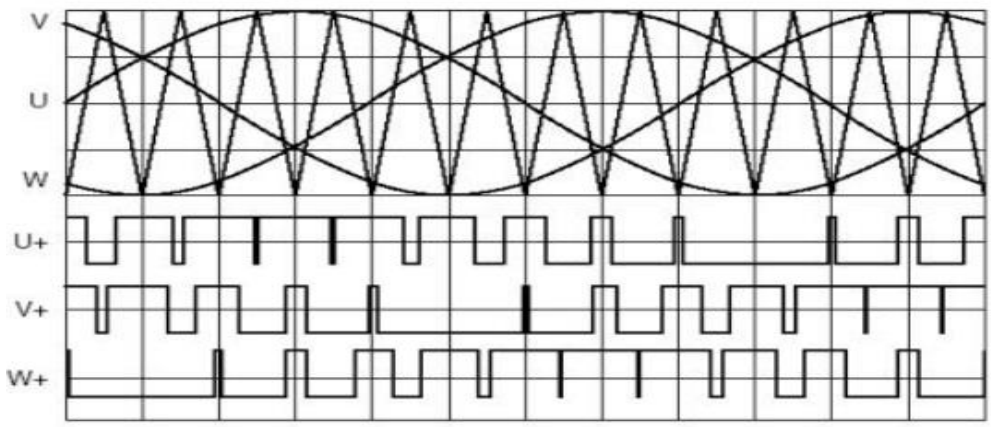

Figure 3. 13Three phase SPWM

In the given block diagram of the three phase inverter with 6 IGBTs is shown in Figure 3.14.

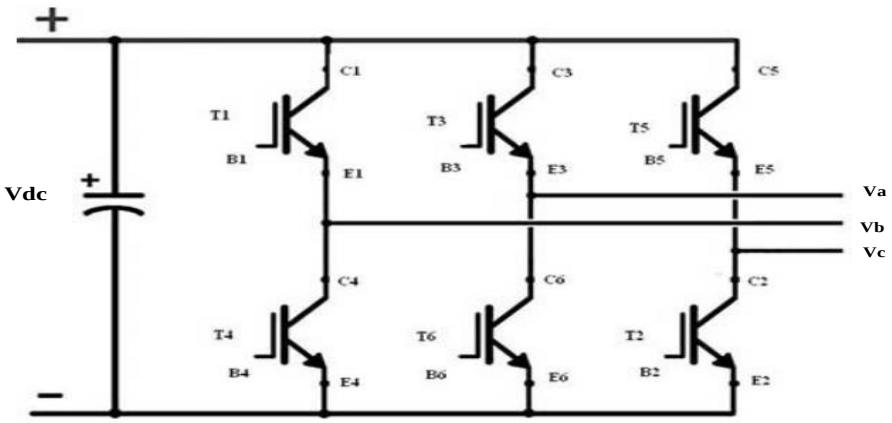

Figure 3. 14Three phase inverter

The inverter is fed by a fixed dc voltage V_{dc} and has three phase-legs each comprising two IGBTs. With SPWM control, the switches of the three phase inverter are implemented by comparing sinusoidal signals and triangular signals. The sinusoidal waves determined the required fundamental frequency of the three phase inverter output, whereas the triangular wave decided the switching frequency of three phase inverter. Each of them transistor conducts for 180 degrees. Three of them transistors conduct at the time in the order of 612,234,345 and so on. When T_1 is switched on, terminal V_b is positive terminal of the DC supply voltage. When T_4 is on, terminal V_b is interconnected to the negative terminal of the input voltage. There are six modes of operation and each mode operates for a period of 60 degrees.

Here sine carriers of PWM are produced by comparing the three references control signals with three triangular carriers' waves. The correlated pulses are generated which are to be fed to the inverter gates devices. The three references control signals are phase shift by an angle $2\pi/3$ and $4\pi/3$ with same amplitude. Two carrier waves are in phase each other with DC voltage. For three-phase SPWM is implemented in matlab Simulink.

3.7. Mathematical Modeling of three phase converter in abc coordinate

3.7.1. 3-Phase Inverter mode modeling

The advantage of the three phase converter is to exchange power in between DC and AC bus. Therefore, this VSC could either operate as rectifier or an inverter without any topology change. A three phase inverter display in Figure.3.15. the complementary switching is assumed. q∈ {0,1}in is the phase x switch state and $q_{x'} = 1 - q_{x.}$ .The sinusoidal duty cycles of switches q_a, q_b, and q_c are Da, D_b, and Dc respectively where V_{dc} is the dc voltage. In the forward direction of the inverter is considered to be from left to right in the figure.3.15.The average model for the inverter is 3-Phase Inverter mode modeling is:

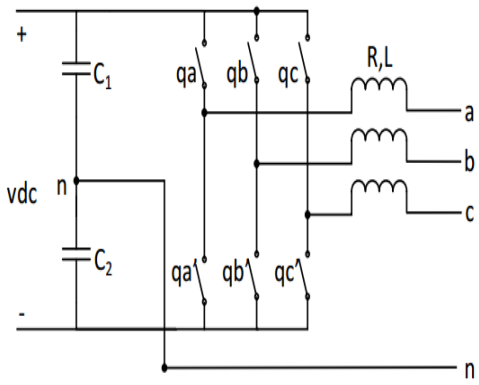

Figure 3. 15 3-phase inverter

$$V_{dc}D_a = L\frac{di_a}{dt} + Ri_a + v_{an} + v_{ng} \text{----(3.11)}$$

$$V_{dc}D_b = L\frac{di_b}{dt} + Ri_b + v_{bn} + v_{ng} \text{----(3.12)}$$

$$V_{dc}D_c = L\frac{di_c}{dt} + Ri_{cb} + v_{cn} + v_{ng} \text{------(3.13)}$$

3.7.2. 3-Phase Rectifier mode modeling

The forward direction of the rectifier is to be left to right in the below figure.3.16. Using analysis similar to that for the inverter, the state average switch mode equations for the rectifier currents are given by:

$$V_{an} = L\frac{di_a}{dt} + Ri_a + (\frac{2}{3}D_a + \frac{1}{3}D_b + \frac{1}{3}D_c)v_{dc} \text{----------(3.14)}$$

$$V_{bn} = L\frac{di_b}{dt} + Ri_b + (\frac{1}{3}D_a + \frac{2}{3}D_b + \frac{1}{3}D_c)v_{dc} \text{----------(3.15)}$$

$$V_{cn} = L\frac{di_c}{dt} + Ri_c + (\frac{1}{3}D_a + \frac{1}{3}D_b + \frac{2}{3}D_c)v_{dc} \text{----------(3.16)}$$

This reduces to:

$$V_{an} = L\frac{di_a}{dt} + Ri_a + (D_a)v_{dc} \text{----------(3.17)}$$

$$V_{an} = L\frac{di_a}{dt} + Ri_a + (D_a)v_{dc} \text{----------(3.18)}$$

$$V_{cn} = L\frac{di_c}{dt} + Ri_c + (D_c)v_{dc} \text{----------(3.19)}$$

In d-q coordinates, this becomes:

$$v_d = Ri_d + L\frac{di_d}{dt} - wLi_q + D_d v_d \text{----------(3.20)}$$

$$v_q = Ri_q + L\frac{di_q}{dt} - wLi_d + D_q v_q \text{----------(3.21)}$$

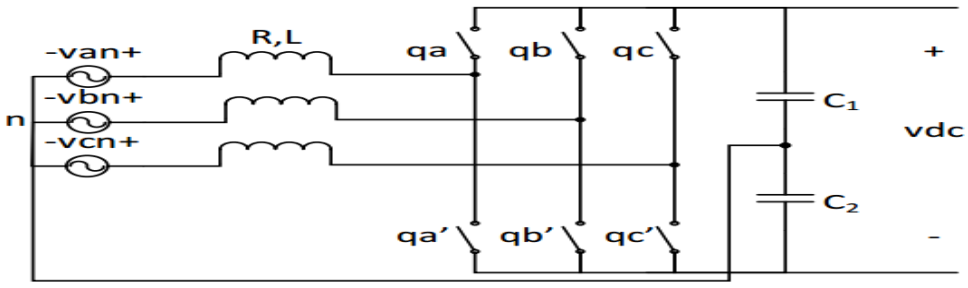

Figure 3. 16 3-phase rectifier without capacitor

3.8. Topologies of DC-DC Converter

The topologies of DC-DC converter are designed to meet specific demand of DC loads. There are different categories of DC-DC converter that can be implemented as switching mode regulation that has been regulate the unregulated DC-voltage with persuasion to applicable exploit voltage through increment or decrement of the values of DC output voltage in implemented by power switching device for PWM switching at a stable frequency which are buck, boost, buck-boost, Single Ended Primary Inductor Converter (SEPIC) and fly back–boost converter [26],[29], [30]. Each converter needs the power switching device for turn-off and turn-on when it is needed. The DC-DC boost converter is runes by Pulse Width Modulation (PWM) switches to control of the converter voltage, frequency and phase delay [27], [31].But in this thesis only we looked DC-DC boost converter.

3.8.1. DC-DC Boost Converter model

Figure3.17 shows circuit topology of DC-DC boost converter model and includes of power switch (M), inductor (L), diode (D), capacitor (C), switching controller and load (R).

This topology specially used for interface connection between low PV array voltages to DC-bus bar. The boost converter will boost up or step up the output voltage to be greater than input voltage. The DC-DC boost converter is used load and the maximum power points tracking (MPPT) controls algorithm. MPPT algorithms were used for producing maximum available power from PV module under a given environmental condition by controlled the duty ratio of DC-DC boost converter. To implemented this converter by using direct duty cycle control (DDC) technique.

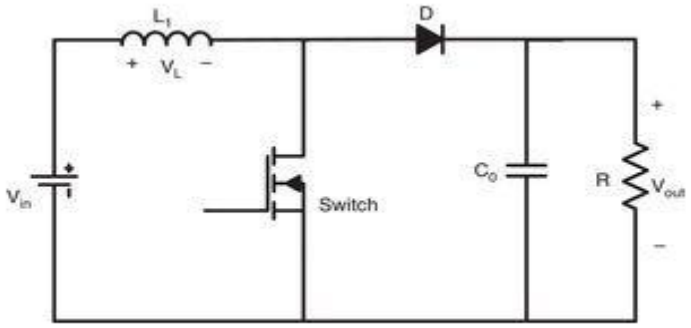

Figure 3. 17Circuit topology of DC boost converter

3.8.2. Direct duty cycle method:

Duty cycle for converter switch was calculated from the previous value of duty cycle. New value of duty cycle varies the converter switch is calculated by increment or decrement the previous values of duty cycle with the help of perturb & observation technique (p&o).

$$V_{out} = \frac{1}{1-D} V_{in} \quad \text{----------(3.22)}$$

$$I_{out} = \frac{1}{1-D} I_{in} \quad \text{----------(3.23)}$$

Where V_{out} = boost converter out put voltage.

I_{out} = boost converter out put currnt.

D = Duty cycle

Table 3. 3Simulation parameters of DC-DC boost converter

No	Parameter	Unit	Values
1	Inductor	Henry	0.9mH
2	Capacitor	Faraday	2mF
3	Switching frequency	Hertz	2KHz
4	Load Resistance	Kilo Ohm	10
5	4 solar cell	Volt	4*3= 12v
6	Duty cycle		D∈ [0,1]

3.9. Dqo transformation

To design a control scheme, it is useful to have constant quantities. To convert abc into constant quantities, dq0 is applied. The Park Transform block changes the time based domain elements of a three phase systems in an abc reference frame to d-axis, q-axis, and zero elements in a rotating reference frame. The block diagram can preserved the active-reactive powers with the system in the abc reference frame by implemented a changing performance of the Park transform. For a balanced system, the zero component is equal to zero.

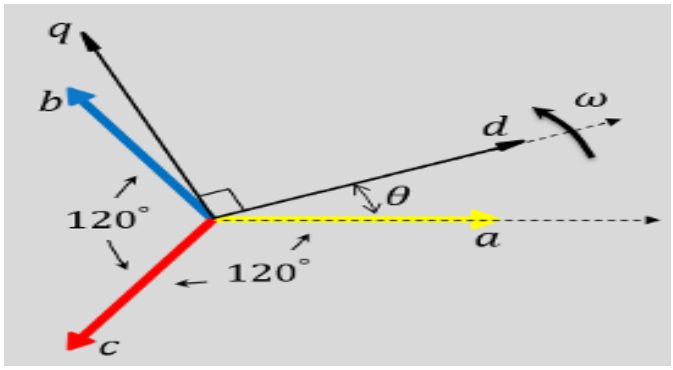

Figure 3. 18Park transformation abc to dq reference.

The dq0 transformation and its inverse are defined as follows:

$$T_\theta = \frac{2}{3}\begin{bmatrix} \cos(\theta) & \cos(\theta - \frac{2\pi}{3}) & \cos(\theta + \frac{2\pi}{3}) \\ -\sin\theta & -\sin(\theta - \frac{2\pi}{3}) & -\sin(\theta + \frac{2\pi}{3}) \\ \frac{1}{2} & \frac{1}{2} & \frac{1}{2} \end{bmatrix} \text{----------(3.24)}$$

$$T_\theta{}^{-1} = \frac{2}{3}\begin{bmatrix} \cos(\theta) & -\sin(\theta) & 1 \\ \cos(\theta - \frac{2\pi}{3}) & -\sin(\theta - \frac{2\pi}{3}) & 1 \\ \cos(\theta + \frac{2\pi}{3}) & -\sin(\theta + \frac{2\pi}{3}) & 1 \end{bmatrix} \text{----------(3.25)}$$

Where the angle θ denoted the references angle or the reference phase. Direct multiplication of these matrices spill that.

$$T_\theta T^{-1}{}_{\theta} = T^{-1}{}_\theta T_\theta = I_{3\times 3}. \text{ ----------(3.26)}$$

The dq0 transformation maps into the three phase signals in abc reference frame to map new variables in a rotating dq0 reference frame and denoted as:

$$X_{abc} = [X_a, X_b, X_c]^T \text{ ----------(3.27)}$$

$$X_{dq} = [X_d, X_q, X_o]^T \text{----------(3.28)}$$

The dq0 transformation is given by:

$X_{dqo} = T_\theta X_{abc}$, where T_θ is the transformation matrix.

3.9.1. Power stage and controller of a three phase VSC

From the controlling point of view, this thesis concerned the most important part of a hybrid DC-AC micro grid is the interlinking three phase voltage source controller (VSC) which links the DC bus with the AC bus. DC load excess of AC supply to DC through the converter and AC load in excess the DC supply has to supply AC load for the application of sensors.

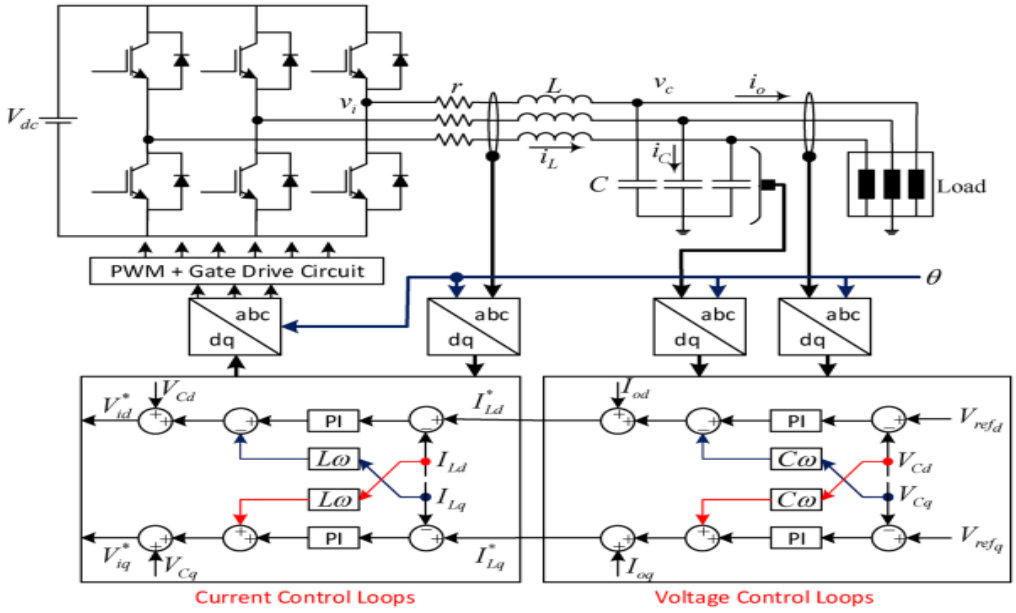

Figure 3. 19Power stage and cascaded form controller of three phase VSC model

The interlinking converter controller consists of three inner loop controllers for both island and grid connected operation of the micro grid. These inner control loops are power controller, voltage controller and current controller. The dynamic modeling for each of the control loops are derived and presented in the succeeding sub sections.

3.9.2. Voltage source converter (VSC) model in the dq reference

The advantage of the three phase converter is to flow power between DC and AC bus. The key purpose of converter is to maintain a stable DC-link voltage. When the converter connects in AC source, it has to supply a given active and reactive power. In PQ control method is implemented for the control of converter. The PQ control is achieved through a current controlled voltage source. Two PI controllers are implemented for real-reactive power control. When resources condition or load values changes, the DC bus bar voltage is settled to stable through voltage controller PI regulations. The inner loop (PI) controller is set as the instantaneous active current i_{dm} reference and the instantaneous reactive-current i_{qm} reference is determined by reactive power set compensation command.

The model of the converter can be characterized in dq coordinate as:

$$L_2 \frac{d}{dt}\begin{bmatrix} i_{dm} \\ i_{qm} \end{bmatrix} = \begin{bmatrix} -R_2 & wL_2 \\ -wL_2 & -R_2 \end{bmatrix}\begin{bmatrix} i_{dm} \\ i_{qm} \end{bmatrix} + \begin{bmatrix} V_{sd} \\ V_{sq} \end{bmatrix} - \begin{bmatrix} V_{cd} \\ V_{cq} \end{bmatrix} \text{----------(3.29)}$$

Where the variables (i_{dm}, i_{qm}), (V_{cd}, V_{cq}) *and* (V_{sd}, V_{sq}) are dq coordinates of three phase currents, voltages of converter and voltage of AC bus respectively.

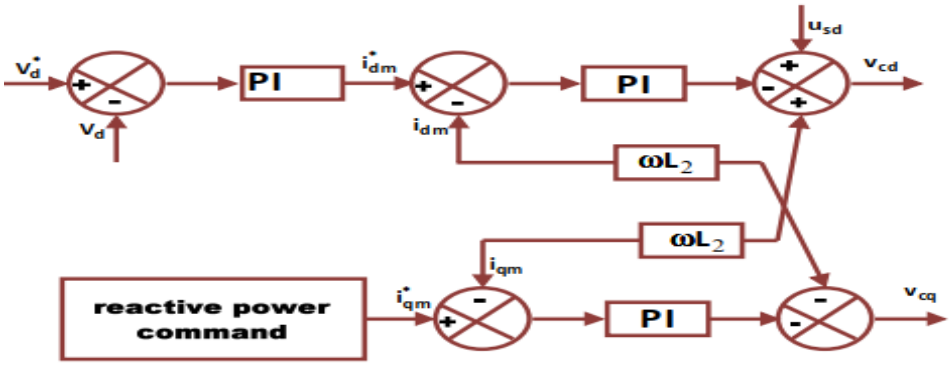

Figure 3. 20Control block diagram of converter

In case of unexpected DC load drop, there is power surplus at DC side and the converter is controlled to flow power from DC to AC side. The active power absorbed by the capacitor C_d leads to rise up of DC-link voltage V_d. The negative error make by the increase of V_d produces a higher active current reference $\mathbf{i^*_{dm}}$ through PI control. A higher positive reference $\mathbf{i^*_{dm}}$ will enforced active current reference $\mathbf{i_{dm}}$ to increase through the inner current control loop. Therefore the power overflow of the DC micro-grid can be transferred to the AC side.

Also a sudden increment of DC load causes the power deficit and V_d drop at the DC grid. The converter is controlled to supply power from the AC to DC side. The positive voltage error happened by V_d drop makes the magnitude of i^*_{dm} increase through the PI control. Since i_{dm} and i^*_{dm} are both negative, the magnitude of i_{dm} is increased through the inner current control loop. Hence power is transferred from AC grid to the DC side.

The system model for such an interconnected between an AC bus and a VSC is shown in figure .3.21below.

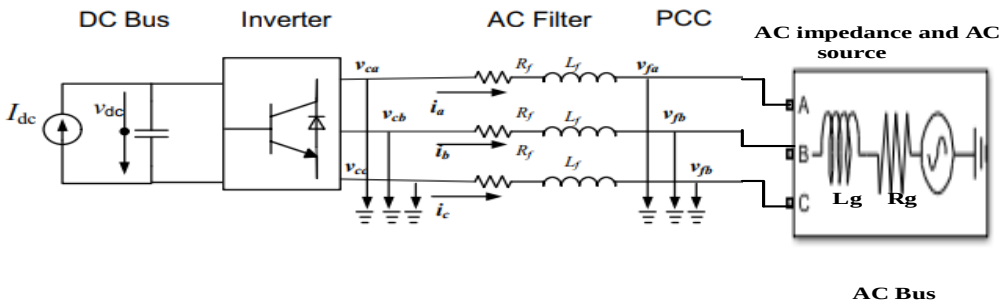

Figure 3. 21 DC source and AC source connection

So we have the dq transformation of equations are:

$$w_g = w_{voltage=} 2\pi f$$

$$V_{cd} = R_f i_d + L_f \frac{di_d}{dt} - w_g L_f i_g + V_{fd} \text{ ----------(3.30)}$$

$$V_{cq} = R_f i_q + L_f \frac{di_q}{dt} - w_g L_f i_d + V_{fq} \text{ ----------(3.31)}$$

The above system model of equations can be represented by the following circuits:

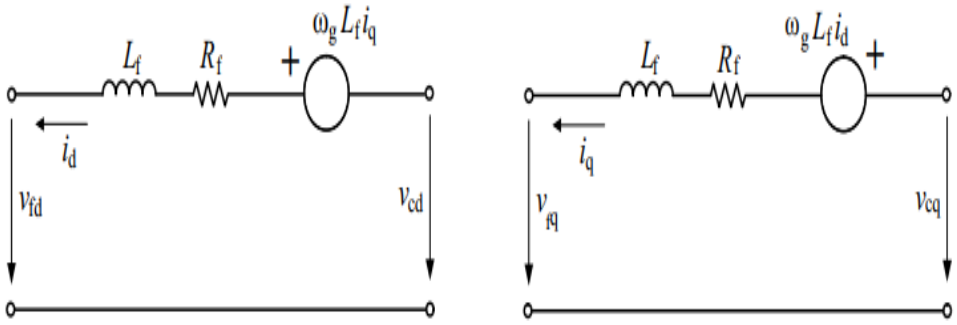

Figure 3. 22Equivalent Circuits for the dq Equations

3.9.3 Inner Loop for AC Current Control

The aim of here to control of the current i_{abc} by applying a voltage V_{abc} with the power converter. Laplace transform of the equations 3.30 and 3.31 is:

$$V_{cd} = (R + sL)i_d - \omega_g L_f i_q + V_{fd} \text{----------(3.32)}$$

$$V_{cq} = (R_f i_q + L)i_q + \omega_g L i_d + V_{fq} \text{----------(3.33)}$$

From which we get:

$$(R + sL)i_d = V_{cd} + \omega_g L_f i_q - V_{fd} \text{----------(3.34)}$$

$$(R_f i_q + L)i_q = V_{cq} - \omega_g L i_d - V_{fq} \text{----------(3.35)}$$

To control the active current i_d, V_{cd} should vary because in the equation R_f, L_f and ω_g are constants. The reference voltages is to be imposed by the invertor (V_{cd} * and V_{cq} *) are obtained from the above equations as:

$$V^*_{cd} = (R + sL)i_d - \omega_g L_f i_q + V_{fd} \qquad V^*_{cd} = \hat{V}_{cd} - \omega_g L_f i_q + V_{fd} \text{----------(3.36)}$$

$$V^*_{cq} = (R_f i_q + L_f)i_q - \omega_g L_f i_d + V_{fq} \qquad V^*_{cq} = \hat{V}_{cq} - \omega_g L_f i_d + V_{fq} \text{----------(3.37)}$$

Where $\hat{V}_{cd}$ and $\hat{V}_{cq}$ are the terms and the outputs of the PI controller. Note that the equations are now decoupled in terms of i_q and i_d.

The system gain is:

$$G(S) = \frac{i_d(s)}{\hat{V}_{cd}(s)} = \frac{i_q(s)}{\hat{V}_{cd}(s)} = \frac{1}{R_f + L_f} \text{----------(3.38)}$$

PI controllers

Proportional-Integral (PI) controllers are one of the most common used types of controllers. A PI controller provides a control signal that has a component proportional to the tracking error of a system and a component proportional to the accumulation of this error over time, and is denoted by the following equation

$$u(t) = K_{p*}e(t) + K_i \int_0^t e(\tau)d\tau \text{ ----------(3.39)}$$

Where $u(t)$ is the control signal and $e(t)$ is the tracking error. In Laplace domain in the above equation can be written as:

$$U(s) = \left(K_P + \frac{K_i}{S}\right) * E(s) \text{ ----------(3.40)}$$

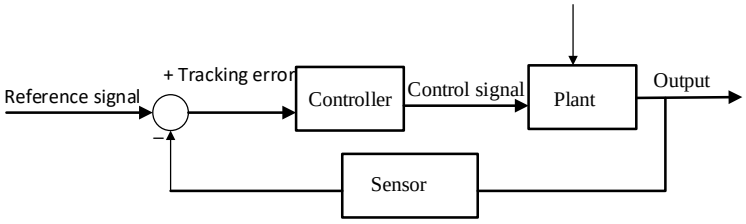

Figure 3. 23 Feedback System with Control

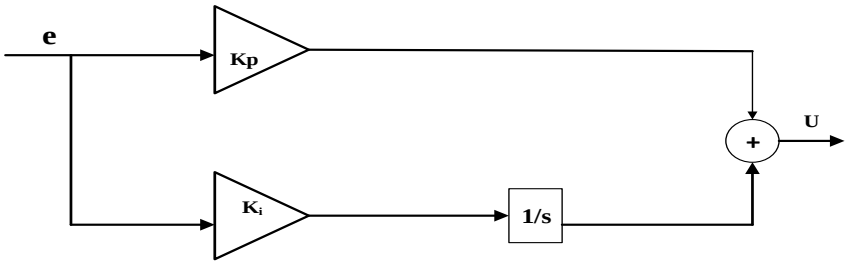

Figure 3. 24PI controller

The control scheme of the currents, using PI controllers, is as follows

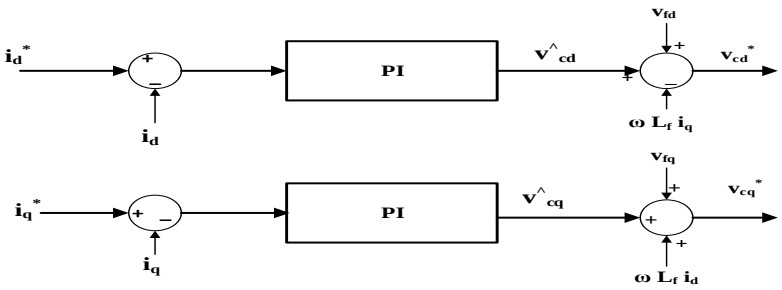

Figure 3. 25Current controller

PI Controller Setting for the Inner Loop:

The system figure of the system and the inner control loop can be drawn as follows

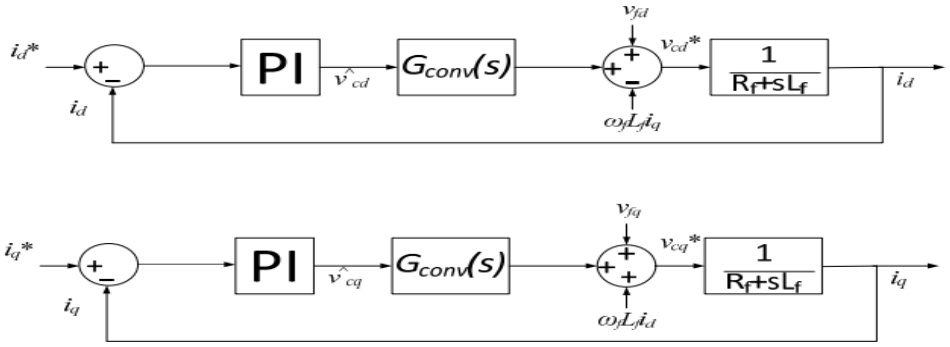

Figure 3. 26Feedback System with Plant and Current Controller

In the current control loop (PI), so that the gain is Gconv(s)=1.Neglecting the disturbances, for transfer function of the above system can be represented as:

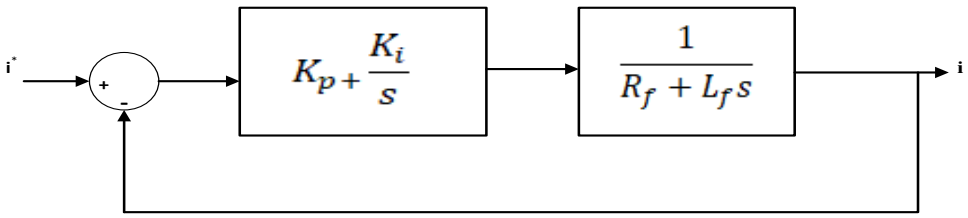

Figure 3. 27 Current Control Closed Loop

The closed loop of the above transfer function and the open-loop transfer function of a feedback system are compared as:

$$G_{closedloop\ (s)} = \frac{G_{open\ loop(S)}}{1+G_{open\ loop(S)}H(s)} \quad \text{----------(3.41)}$$

Here H(s) =0

$$G_{open\ loop(S)} = \frac{K_p S+K_i}{S(R_f+L_f)} \quad \text{----------(3.42)}$$

So the closed loop of the above transfer function is given as:

$$G_{closedloop\ (s)} = \frac{K_p s + K_i}{L_f s^2 + (R_f + K_P) S + K_i} \text{ ----------(3.43)}$$

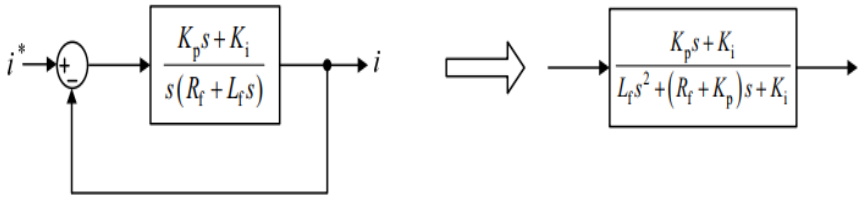

Figure 3. 28 Open loop and Closed Loop Gain

The denominator of the closed loop of transfer function is, divide the whole terms by $\mathbf{L_f}$.

$$L_f s^2 + (R_f + K_P) S + K_i = 0 \text{ , give as } \quad s^2 + \left(\frac{R_f + K_p}{L_f}\right) s + \frac{K_i}{L_f} \text{ ------(3.44)}$$

Comparing the above equation with the characteristic second order equation

$$s^2 + 2\xi w_n s + w_n{}^2 = 0 \text{ ----------(3.45)}$$

After equate we get the parameters:

Where $w_n = \frac{-\ln(\varepsilon)}{\xi t_s}$ $\qquad K_P = 2\xi w_n L_f - R_f$ ----------(3.46)

$\xi = \sqrt{\frac{\ln^2(M_p)}{\ln^2 M_p + \pi^2}} =$ $\qquad K_i = L_f w_n{}^2$----------(3.47)

3.9.4. The Outer Loop for DC Voltage Control

The outer loop controller (PI) is for voltage of the DC bus. The DC voltage control is implemented through the control of power exchanged by the converter with the AC source. Increasing or decreasing the worked in power with respect to the power produced by the DC system decreases or increases the voltage level to keep it under control. The outputs for the DC voltage controller (PI) deliver the reference current for the inner loop. The constant current source I_{dc} can be modeled as a constant power source, value:

$$I_{dC} = \frac{P^*}{V_{dc}} \text{----------(3.48)}$$

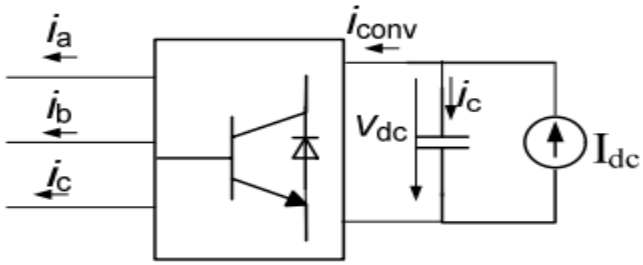

Figure 3. 29Currents at the Inverter

The current in the DC bus capacitor is given by:

$$i_c = C\frac{dv_{dc}}{dt} = I_{dc} - i_{conv} \text{ ----------(3.49)}$$

We want to carry on a constant DC side voltage, so that $\frac{dv_{dc}}{dt} = 0$ implies$I_{dc} = i_{conv}$

And $P_{dc} = V_{dc} * I_{dc}$ ----------(3.50)

Using the power balance on the AC side and DC side:

$P_{dc} = P_{AC}$, where $P_{AC} = 3/2(V_{cd}i_d + V_{cq}i_q)$----------(3.51)

We can observe that if the active current i_d is regulated, we can control the bus voltage V_{dc}.

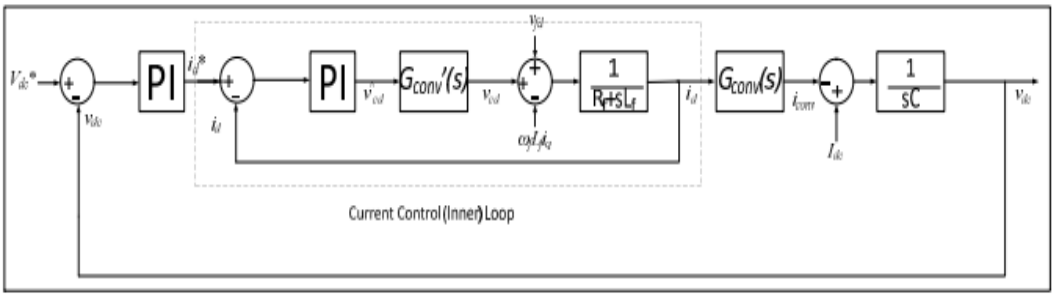

Figure 3. 30 Voltage control (outer loop)

PI Controller Setting for the Outer Loop

$$i_c = C\frac{d_{v_{dc}}}{dt} = C\frac{d_{v_c}}{dt} \text{----------(3.52)}$$

This in Laplace domain gives as:

$$V_c(s) = \frac{1}{Cs} I_c(s) \text{----------(3.53)}$$

A PI controller is implemented with the following transfer function:

$$G_{PI} = K_p + \frac{K_i}{S} \text{----------(3.54)}$$

The open loop of the transfer function for voltage control loop (PI), neglecting the disturbances and the inner loop is:

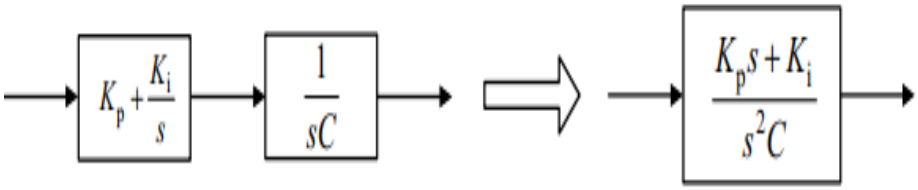

Figure 3. 31 Voltage Control Open Loop

As the relation between open loop transfer function and closed loop of the transfer function for a feedback system is given as;

$$G_{closed\ loop\ (s)} = \frac{G_{open\ loop(S)}}{1+G_{open\ loop(S)}H(s)} \text{----------(3.55)}$$

Where H(s) is the loop gain, and for this case is 1.The equation for the closed loop is written as:

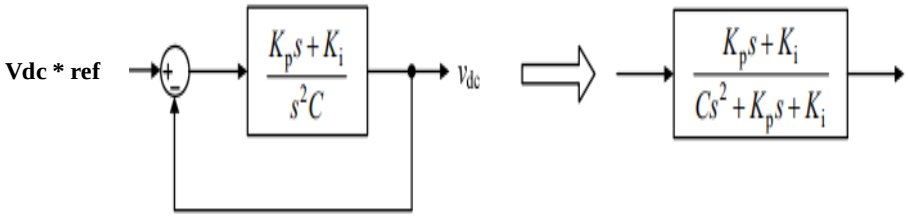

Figure 3. 32Voltage control closed Loop

To attain the poles of the system, we put the denominator of the system equation equal to zero. Divide the whole terms by C.

$$Cs^2 + K_P s + K_i = 0 \text{ , which gives } s^2 + \frac{K_P s}{C} + \frac{K_i}{C} = 0 \quad \text{----------(3.56)}$$

Equating the coefficient with the equation second order $s^2 + 2\xi w_n s + {w_n}^2 = 0$

We get the parameter $K_P = 2\xi w_n C$ and $K_i = C{w_n}^2$

Where ξ and ω_n are gained the same way as in that of the current PI.

The dynamics of the outer loop control is greater than the inner loop. The internal loop is designed to achieve short settling times, and the external loop is designed keeping in mind the stability and regulation, and it is designed to be slower than the internal current loop.

This also implies we can consider both loops to be decoupled. ω_n for the outer loop should be tuned to be at least three to five times slower than the inner loop time constant.

3.10. Power flow in terms of dq0 quantities

The dq*0* transformation and its inverse are defined as follows:

$$T_\theta = \frac{2}{3}\begin{bmatrix} \cos(\theta) & \cos(\theta - \frac{2\pi}{3}) & \cos(\theta + \frac{2\pi}{3}) \\ -\sin\theta & -\sin(\theta - \frac{2\pi}{3}) & -\sin(\theta + \frac{2\pi}{3}) \\ \frac{1}{2} & \frac{1}{2} & \frac{1}{2} \end{bmatrix} \text{----------(3.57)}$$

$$T_\theta{}^{-1} = \frac{2}{3}\begin{bmatrix} \cos(\theta) & -\sin(\theta) & 1 \\ \cos(\theta - \frac{2\pi}{3}) & -\sin(\theta - \frac{2\pi}{3}) & 1 \\ \cos(\theta + \frac{2\pi}{3}) & -\sin(\theta + \frac{2\pi}{3}) & 1 \end{bmatrix} \text{----------(3.58)}$$

Where the angle θ is reference angle or the reference phase. Direct multiplication of these matrices reveals that.

$$T_\theta T^{-1}{}_\theta = T^{-1}{}_\theta T_\theta = I_{3\times 3}. \quad \text{----------(3.59)}$$

The dq0 transformation mapping three phase signals of the abc reference frame into new variables in a rotating of dq0 reference frame.

Denotes:

$$X_{abc} = [X_a, X_b, X_c]^T \quad \text{----------(3.60)}$$

$$X_{dq} = [X_d, X_q, X_o]^T \quad \text{----------(3.61)}$$

$X_{dqo} = T_\theta X_{abc}$, where T_θ is the transformation matrix.

Then a fundamental property of the dq0 transformation is that it maps balanced three-phase signals to constants .The three-phase voltage source modeled as a phase shift 120^0.

$$V_a = A\cos(w_s t), \quad \text{----------(3.62)}$$

$$V_b = A\cos\left(W_s t - \frac{2\pi}{3}\right), \quad \text{----------(3.63)}$$

$$V_c = A\cos(w_s t + \frac{2\pi}{3}) \quad \text{----------(3.64)}$$

$\theta = w_s t$ where is w_s is the frequency of infinite bus. Applying the inverse transformation T_θ^{-1} with $\theta = w_s t$ *le*ads to:

$$\begin{bmatrix} V_a \\ V_b \\ V_c \end{bmatrix} = \begin{bmatrix} \cos(w_s t) & -\sin(w_s t) & 1 \\ \cos(w_s t - \frac{2\pi}{3}) & -\sin(w_s t - \frac{2\pi}{3}) & 1 \\ \cos(w_s t + \frac{2\pi}{3}) & -\sin(w_s t + \frac{2\pi}{3}) & 1 \end{bmatrix} \begin{bmatrix} A \\ 0 \\ 0 \end{bmatrix} \quad \text{----------(3.65)}$$

Where $V_d = A$, $V_q = 0$, $V_0 = 0$

The sinusoidal signals of in abc references are mapped to constant signals in the dq0 reference frame.

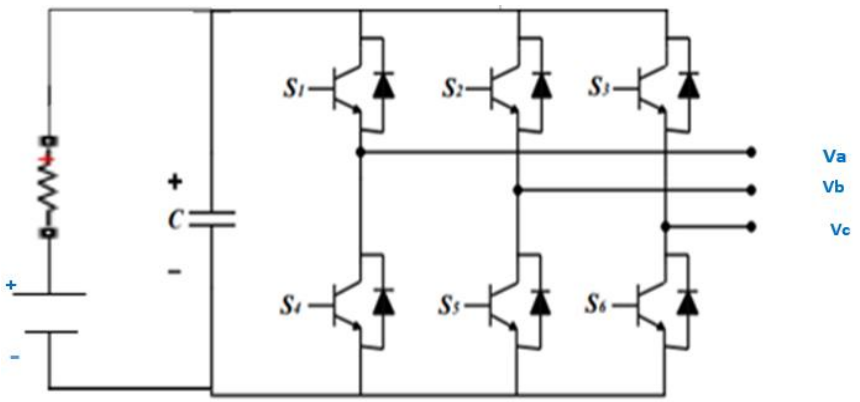

Figure 3. 33Three phase inverter

In a general three-phase inverter unit as described in Figure.3.33.The instantaneous power flowing from the unit into the network at time t is:

$$P_{3\varphi}(t) = V_a(t)i_a(t) + V_b(t)i_b(t) + V_c(t)i_c(t): \text{----------(3.66)}$$

Rewrite this equation as:

$$P_{3\varphi} = [V_a \quad V_b \quad V_c]\begin{bmatrix} i_a \\ i_b \\ i_c \end{bmatrix}` = \left(T_\theta{}^{-1}\begin{bmatrix} V_d \\ V_q \\ V_0 \end{bmatrix}^T T_\theta{}^{-1}\right)\begin{bmatrix} i_d \\ i_q \\ i_o \end{bmatrix} \text{----------(3.67)}$$

$$P_{3\varphi} = [V_d \quad V_q \quad V_o]\,(T_\theta{}^{-1})^{\mathrm{T}}\,T_\theta{}^{-1}\begin{bmatrix} i_d \\ i_q \\ i_o \end{bmatrix} \text{----------(3.68)}$$

$$(T_\theta{}^{-1})^{\mathrm{T}}\,T_\theta{}^{-1} = \frac{3}{2}\begin{bmatrix} 1 & 0 & 0 \\ 0 & 1 & 0 \\ 0 & 0 & 2 \end{bmatrix} \text{----------(3.69)}$$

$$P_{3\varphi} = \frac{3}{2}[V_d \quad V_q \quad V_o]\begin{bmatrix} 1 & 0 & 0 \\ 0 & 1 & 0 \\ 0 & 0 & 2 \end{bmatrix}\begin{bmatrix} i_d \\ i_q \\ i_o \end{bmatrix} = \frac{3}{2}[V_d i_d + \quad V_q i_q + \quad 2V_o i_o] \text{------(3.70)}$$

For power factor Vq=0 and V_0=0, then $p_{3\emptyset} = \frac{3}{2} v_d i_d$.

Then the power flow from AC source to DC supply to interchange the polarity of after dqo reference V_d positive and I_d negative.

3.11. Load demand identify using fuzzy logic controller

Fuzzy logic supposition is studied as a mathematical approach combining multi-valued logic, probability theory, and artificial intelligence to replicate the human approach in reaching the solution of a specific problem by using approximate reasoning to relate different data sets and to make decision. The execution of Fuzzy Logic Controller (FLC) is well validated in the field of control concept of theory since it provided robustness to dynamic system to the parameter variations besides improved transient and steady state execution. The proposed FLC scheme exploits the implicitly of the Mamdani type fuzzy systems that are implemented in the design of the controller.

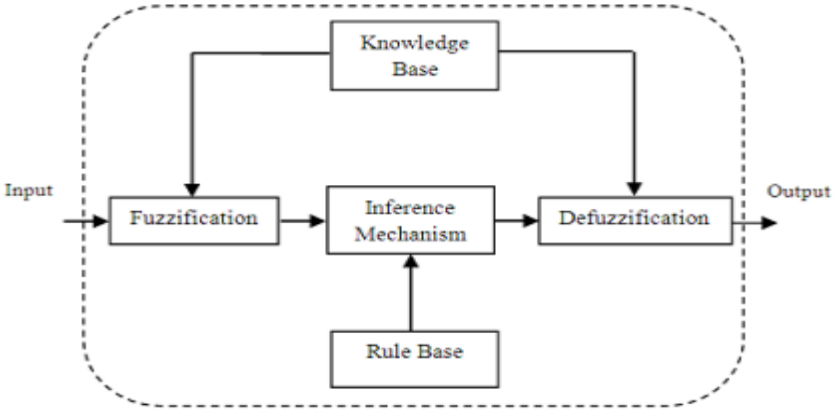

Figure 3. 34Schematic representation of Fuzzy Logic Controller.

The fuzzy logic based control scheme (Figur.3.34) can be divides to the main four functional groups such as Knowledge base, Fuzzifications, Inference engine and the Defuzzification. The knowledge based is includes of data bases and rule bases.

Database includes of input memberships and output memberships function and this provides information delivered for fuzzification and defuzzification operations. The rule-base includies of a set of human decision linguistic rules like the fuzzified input variables to the required control actions. Fuzzification changes a crisp input signals, error (e), and change in error (ce) into fuzzified stages that can be isolated in the level of memberships in the fuzzy sets. The inference engine makes the collection of human decision linguistic rules to change the input signals to fuzzified output. Finally, the defuzzification stage changes the fuzzified outputs into control signals by implementing the output membership variables, this leads the system acts like the change in the control input (u). The typical input membership functions for error and change in error are shown in figure.3.35 and figure.3.36 respectively, whereas the output membership variables for change in control input is shown in Figue.3.37.The output generated with the fuzzy logic controller (FLC) must be crisp which issued to control the load demand from AC grid, DC gride and thus accomplished by the defuzzification block. Many defuzzification methods are functional in the weighted average criterion, the centroid method and mean-max membership. In this thesis the defuzzification methodes implemented based on the centroid method. Fuzzy logic controllers are proposed to control a three phase inverter for DC-AC connected system based on their load demands. The FLC was used to identify the AC load voltage and DC load using voltage sensor. The output of FLC was used to control the active power injected to compare AC load and DC load to set V_{ref} and V_d into the internal PI controller. The study investigated different renewable energy is design to satisfy the energy demand and to increase the power efficiency of the village local home. This study should identify collect the load demand based on the consumption, analyzed relevant data, information to examine and select the most suitable systems configuration, recommend necessary action, necessary measures that configure a system to accommodate the current and near future electrical energy demand for the village and local home. The table 3.4 shows the load demand on the total demand in DC bus bar is 142kw and the total load demand in the AC bus bar is 210kw.

Then next based on the load demand to limit the range of power flow on both side and this is implemented by fuzzy member function.

In the given below the total Load in watt identification on DC bus bar and AC bus bar in some local area home.

Table 3. 4The load demand on DC bus bar and load demand on AC bus bar in

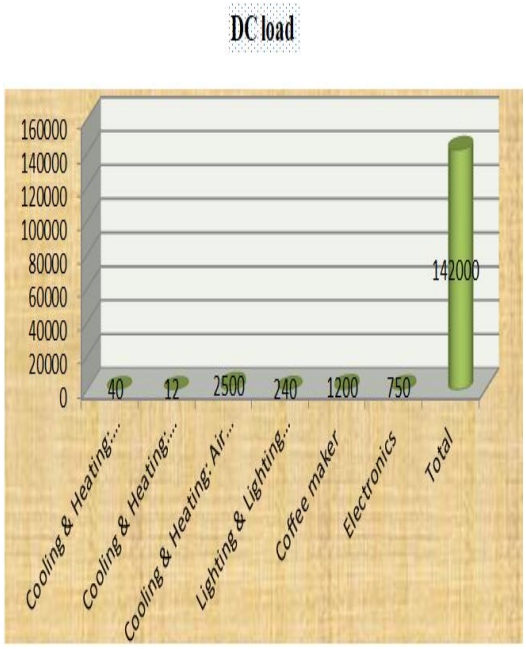

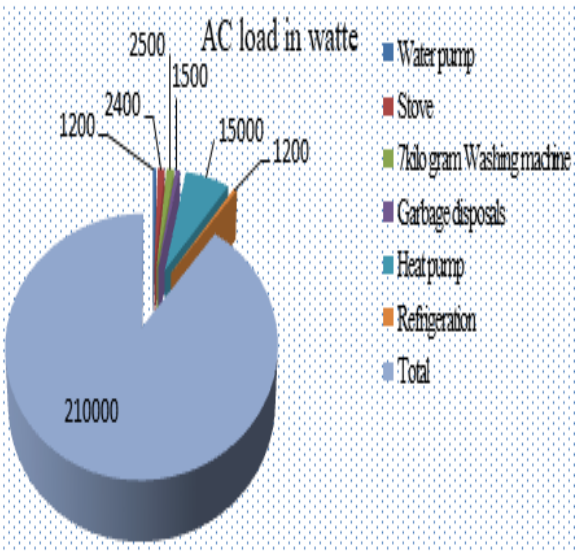

In general to control the power flow on both side loads balancing is the process to maintain the outputs in certain limits and load balancing is to maintain the system load in specific limits or as per the system requirement and the measured value from the system. Now, the input is named Load (kW) to indicate total phase load for DC load and AC load whereas the output is named Change (kW) to calculate the total change of load for each.

Table 3. 5 Fuzzy logic controller DC load power range

Input load Description	Fuzzy logic Linguistic term	Power load in kW
DC small	DS	<80
DC medium	DM	120-140
DC big	DB	140-160
DC large	DL	200-210

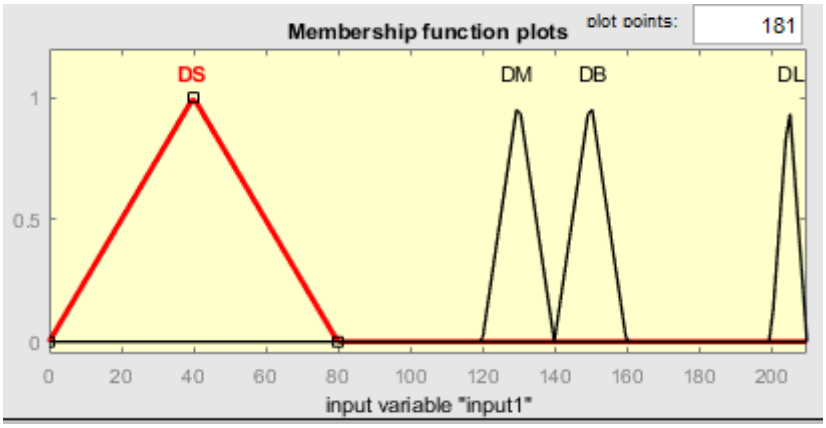

Figure 3. 35Fuzzy logic controller Member function input-1 DC load variable.

Table 3. 6Fuzzy logic controller AC load power range

Input Load Description	Fuzzy logic Linguistic term	Power load range in Kw
AC small	AS	80-100
AC medium	AM	100-120
AC big	AB	160-180
AC large	AL	190-240

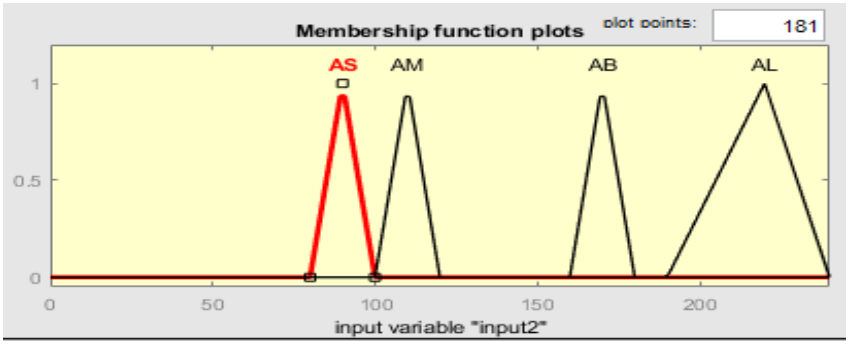

Figure 3. 36Member function input-2 AC load variable

Table 3. 7Fuzzy logic controller Output power load.

Output Load Description	Fuzzy logic Linguistic term	Power load range
DC medium	DM	120-140
DC big	DB	140-160
AC medium	AM	100-120
AC large	AL	190-240

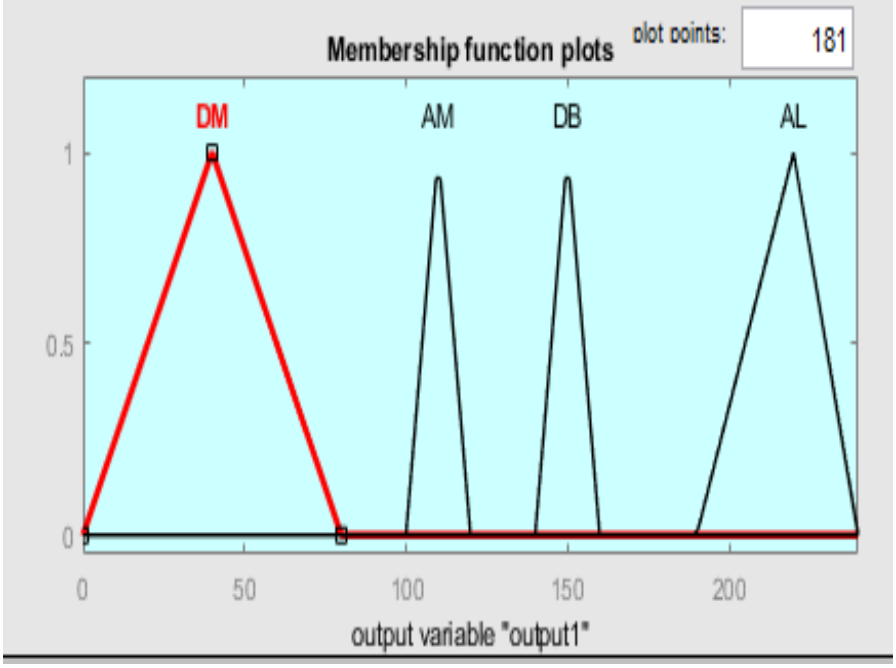

Figure 3. 37Fuzzy logic controller Member function output variable.

CHAPTER -FOUR

4. SIMULATION RESULTS AND DISCUSSION.

A DC-AC micro grid whose parameters are given in table 3.1, 3.2 and 4.1 is simulated using MATLAB/SIMULINK environment. Along with the hybrid micro grid, the implementation of the wind turbine, photovoltaic system is analyzed. The solar irradiation, cell temperature and wind speed, load demand and power flow on both side are also taken into consideration for the study of hybrid DC-AC micro grid. To analyze the performance of system we have designed a Matlab/Simulink model voltage source inverter as in dq reference frame shown in the figure.4.1and the overall performance analysis is done using simulated results which are found using MATLAB.

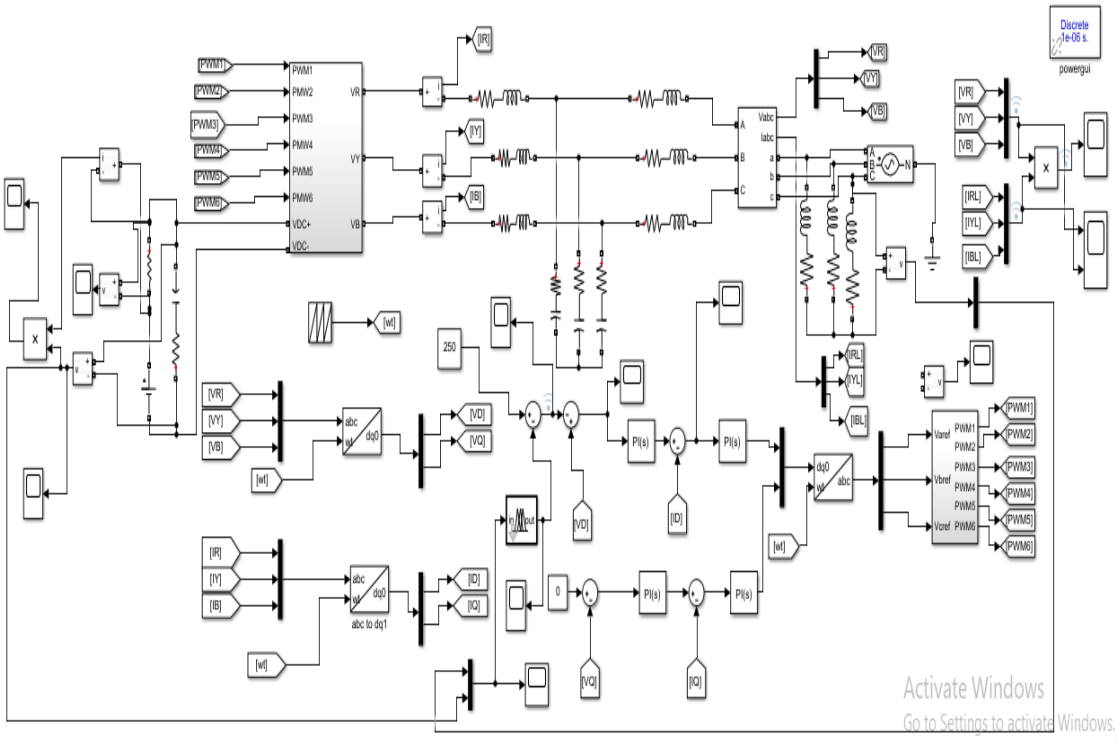

Figure 4. 1Matlab schematic diagram for cascaded control simulation

Table 4. 1 Parameters used for cascaded control simulation

No	Parameters	unit	value
DC-Micro grid (DC-DC boost converter)			
1.	Inductor	Millihenery	0.9mH
2.	Capacitor	Millifaraday	2mF
3.	Switching frequency	Kilo Hertz	2KHz
4.	DC load	Kilo ohm	10kΩ
5.	Four solar cell	Volt	3*4=12v
6.	Output power	Kilo watt	142kw
6.	Duty cycle		D∈ [0,1]
	Interlinking voltage source converter		
7.	Input voltage PV boost V_{dc}	volt	160v
8.	Switching frequency	Kilohertz	10kHz
9.	Rated power	Kilo volt ampere	100KVA
10.	PI controller voltage regulator		K_p=0.1,k_i=100
11.	PI controller current regulator		K_p=30,k_i=200
	Low pass filter		
12.	Filter resistance	Ohm	R_f =0.05Ω
13.	Filter inductor	Millihenery	5mH
14.	Capacitor	Millifaraday	0.1mF
	AC micro grid		
15	Wind turbine power output	Kilo watt	250Kw
16	AC load	Kilo watt	210Kw
17	Frequency	Hertz	50Hz

4.1. Simulation result DC micro-grid.

4.1.1. Simulation of PV array

Figure (4.2.)-(4.7.) represents I-V, P-V, P-I characteristics with variation in temperature and solar irradiation. The nonlinear nature of PV cell is mark in the figures below, i.e., the output current and power of PV cell depend on the cell's terminal operating voltage and temperature, and solar irradiation as well.

Figures 4.2. and 4.3. show that with increase of cell's working temperature, the current output of PV module increases, whereas the maximum power output reduces. Since the increase in the output current is much less than the decrease in the voltage, the total power in general decreases at high temperatures.

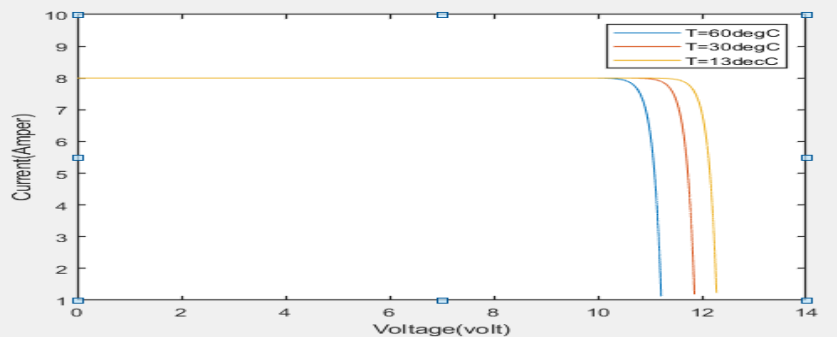

Figure 4. 2 I-V output characteristics of PV array for different temperatures

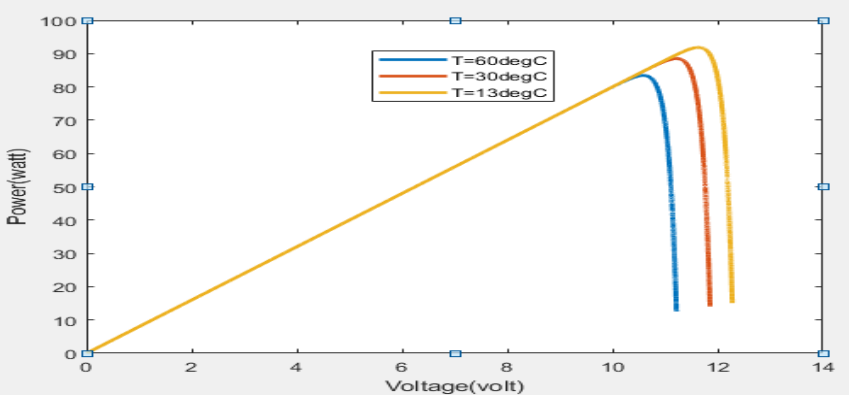

Figure 4. 3P-V output characteristics of PV array for different temperatures

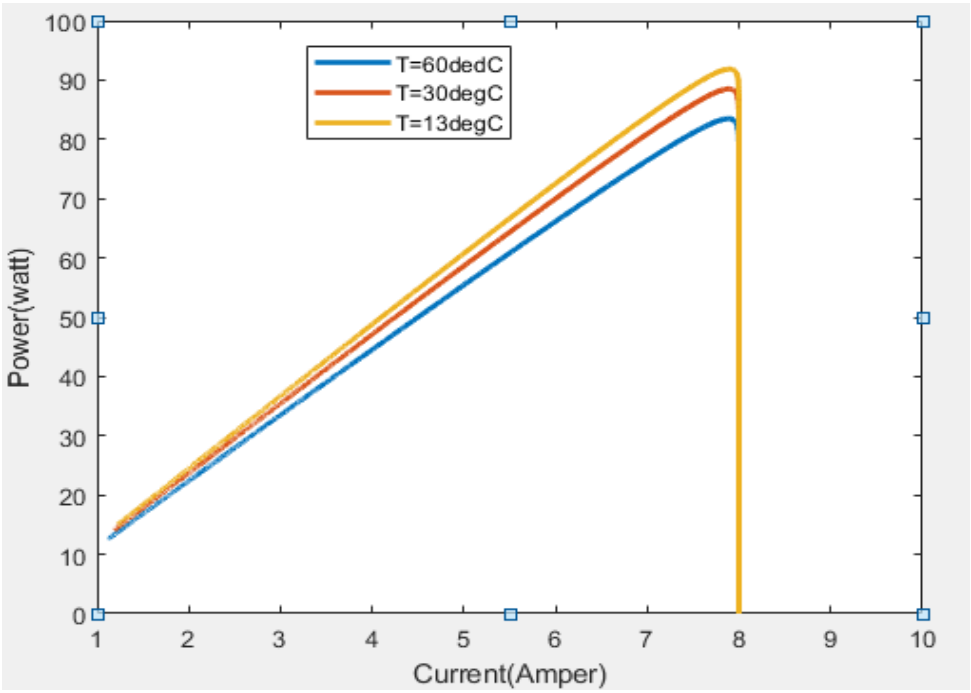

Figure 4. 4P-I output characteristics of PV array for different temperatures

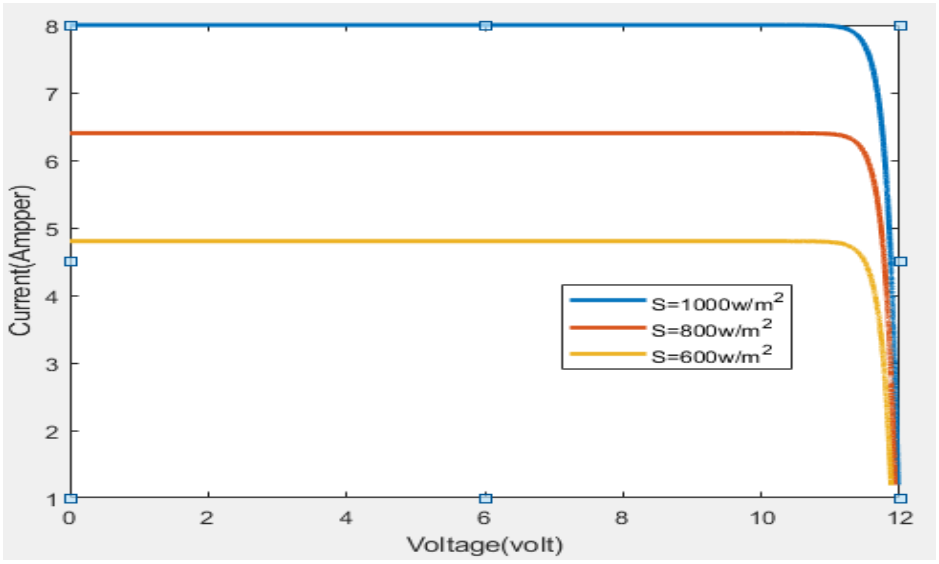

Figure 4. 5I-V output characteristics of PV array for different irradiance levels

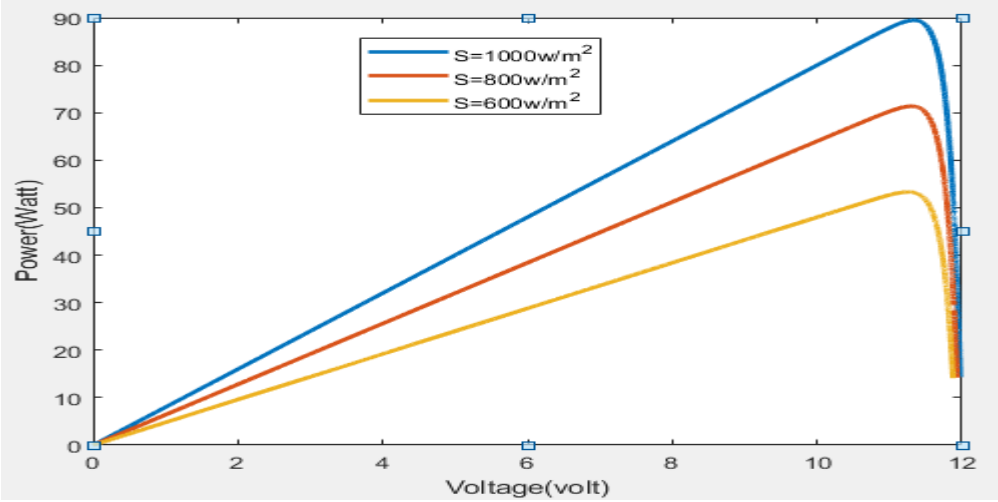

Figure 4. 6P-V characteristics of PV array for different irradiance levels

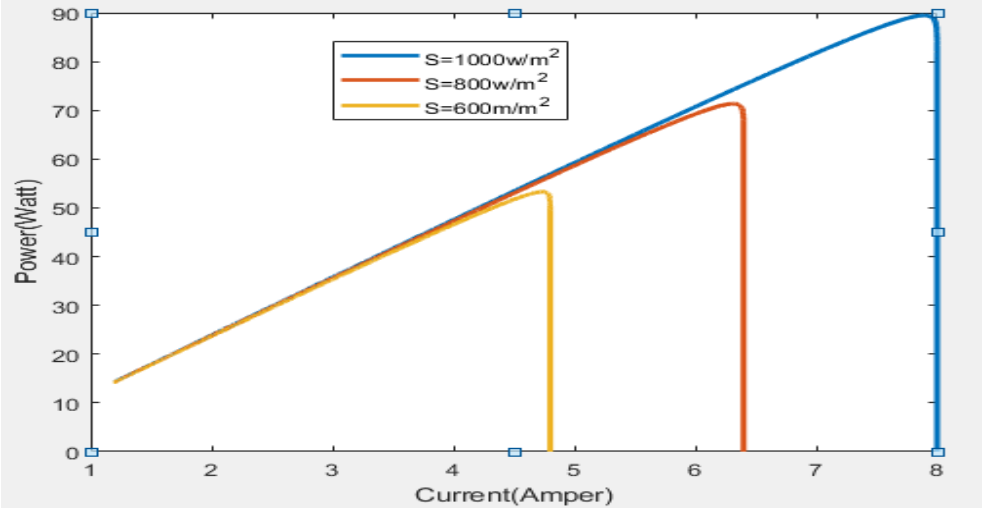

Figure 4. 7P-I characteristics of PV array for different irradiance levels

Figures (4.5) and (4.6) show that with increase of solar irradiation, the current output of PV module increases and also the maximum output power. The reason behind it is the open circuit voltage is logarithmically depended on the solar irradiation; however the short-block current is more of directly correlated to the radiant intensity.

4.1.2. Simulation of DC-DC boost converter

The dc micro grids the main components of are PV array, DC-DC boost converter, load and the MPPT control algorithm. Boost converters for PV applications are the ability to produce 160volt output from a low voltage input 12volt and 142kw output power to vary the parameter of inductor, resistor and control of duty cycle.

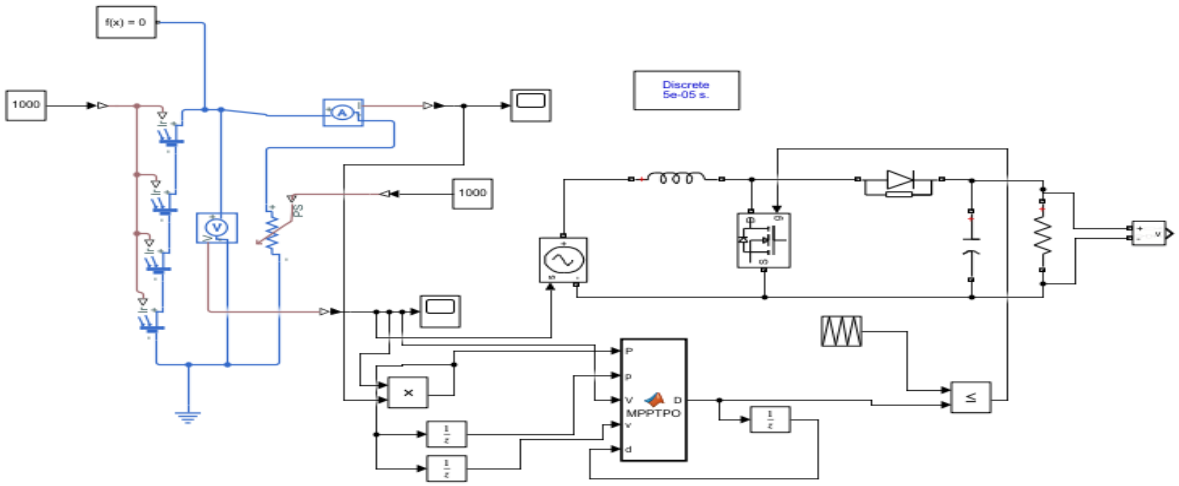

Figure 4. 8Matlab Simulink model of DC-DC boost converter.

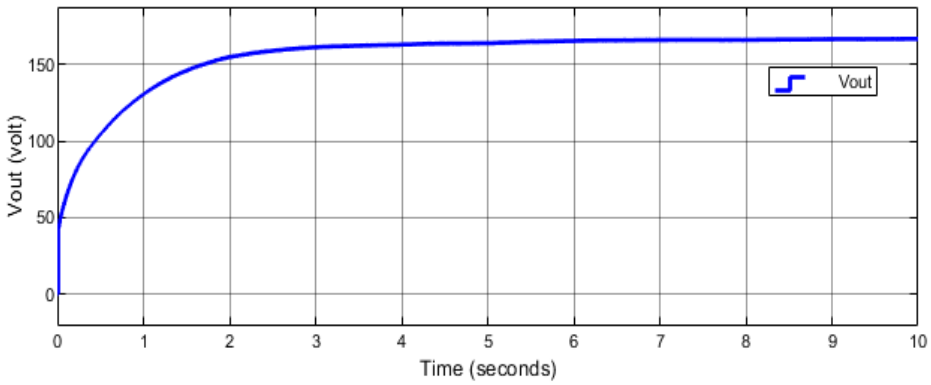

Figure 4. 9The output voltage of DC-DC boost converter.

4.2. Simulation result AC micro-grid.

4.2.1. Simulation of wind turbine.

The response of wind speed three phase rotor voltage are in the figures (4.10.) - (4.12.) Here the value of wind speed varies between 0.73 to 1.2 pu. The output rotor voltage value is 220V.

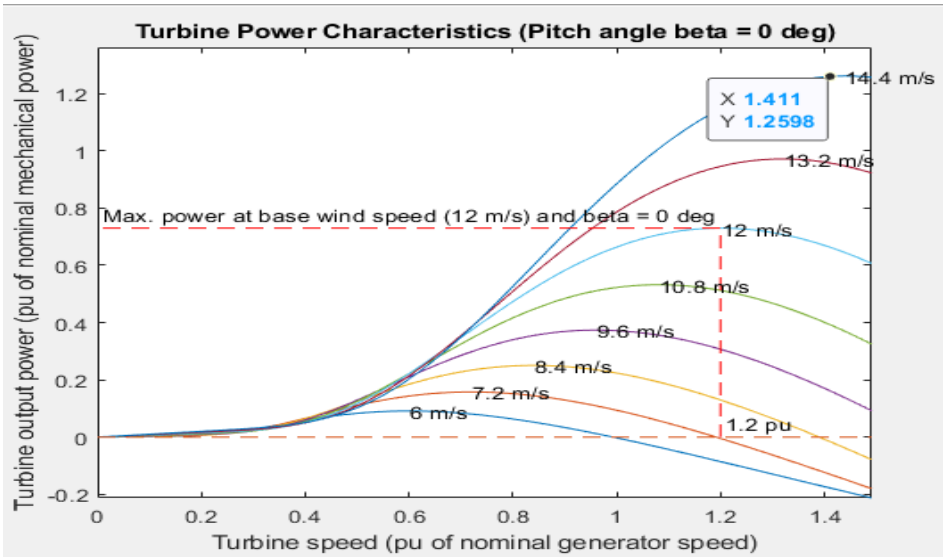

Figure 4. 10 Response of wind speed and Max. Power at base wind speed.

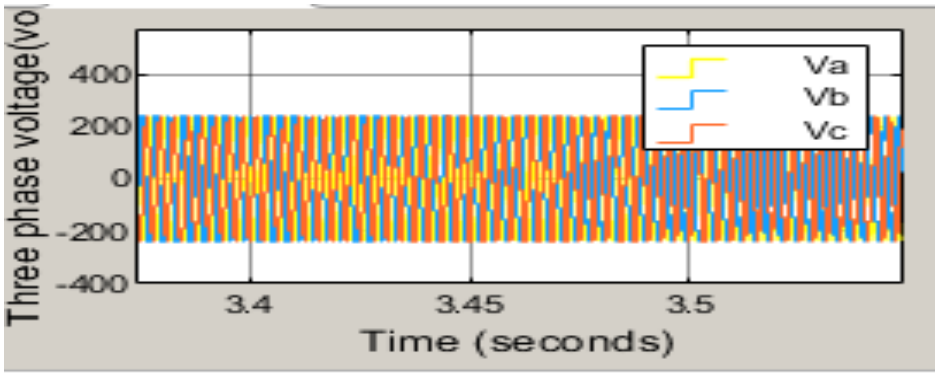

Figure 4. 11Three phase rotor voltage of wind turbine.

In Figure.4.11.and figure.4.12.shows that the output value of voltage and the power are depended on the rotor wind speed with external wind speed at 400m/sec.

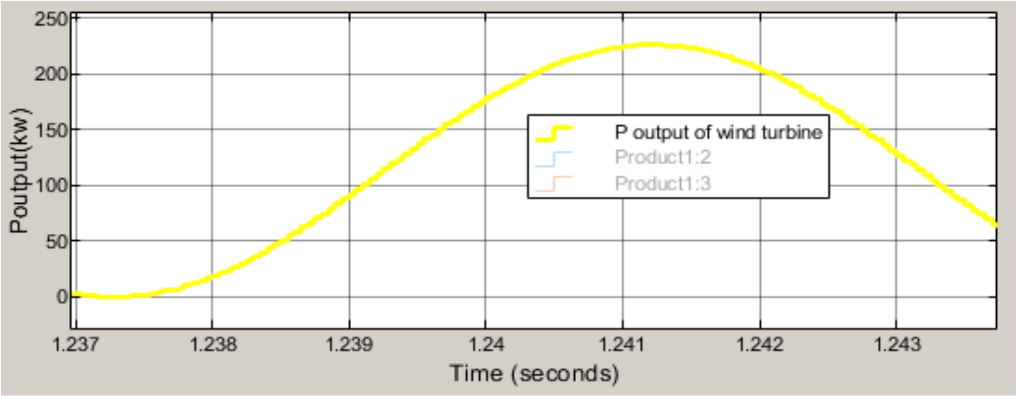

Figure 4. 12 the output power of wind turbine

4.3. Simulation results of DC-AC micro grid

The various characteristics of the hybrid micro grid are represented by the figures (4.13 – 4.21) implemented in dq reference frame. Here the micro grid operates DC-AC interfacing voltage source converter. In this case, the converter regulate in the PQ mode and power is balanced case, no need of power passes through the converter .If the DC load excess, then the AC has supply to the DC load through the converter to sense DC load current. AC load in excess the DC supply to the AC load at the reverse of Voltage source inverter using voltage sensor application and with small in power factor. The table below the parameter of VSI and the overall parameter value in table 4.2.

Table 4. 2The parameters of matlab simulation voltage source inverter.

No	Parameter	Values
1	Rated power	100KVA
2	Input voltage V_{dc}	160-800V
3	Switching frequency	10KH
4	PI controller voltage regulator	Kp=0.1 ,Ki =100
5	PI controller current regulator	Kp=30 ,Ki=200

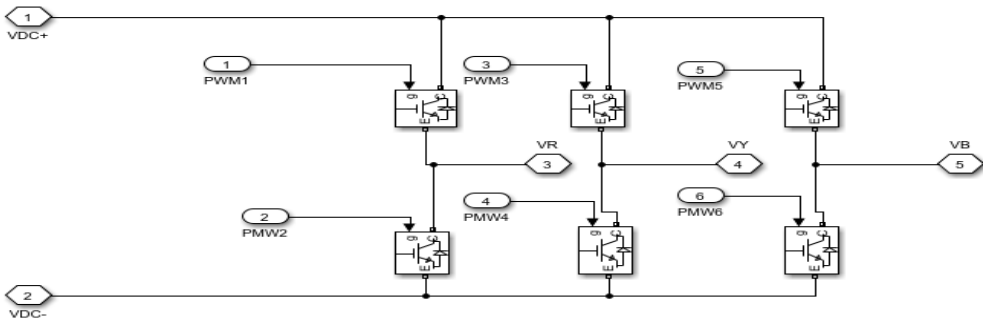

Figure 4. 13Matlab schematic modeling of voltage source inverter

Case.1. If DC bus bar and AC they are balanced load on both side in this case no need of power flow in both side and to feed itself.

Case.2. AC load in excess means the high inductive load happen for this case to sense the low power factor happen in the AC bus. So, require more power, then the DC supply to supply to AC load for this case the operation act as an inverter using SPWM (modulation index) method. The gate pulses given to the three phase inverter are shown from Figure 4.14 up to 4.16. The frequency of carrier signals is kept 10 KHz whereas reference is varied constant value. The DC input PV array voltage is kept as 160V. The AC load resistor values are chosen the range 50 ohm-500 ohm and inductive load 200mH.

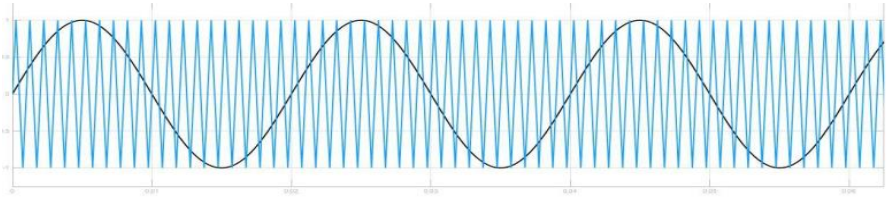

Figure 4. 14Gate pulses for T1

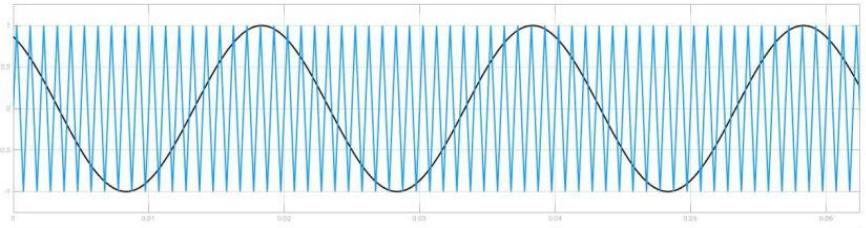

Figure 4. 15Gate pulse for T3

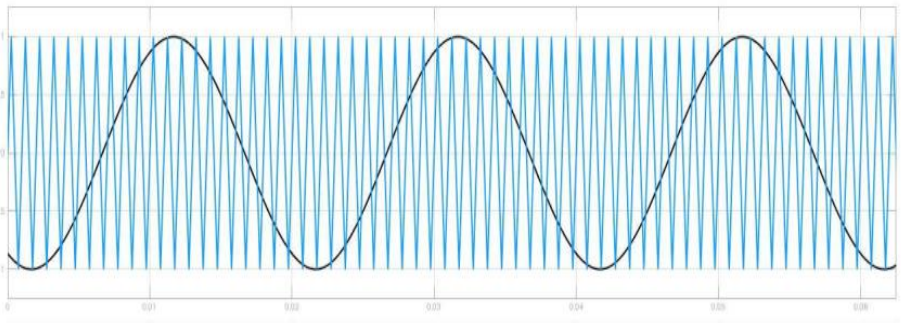

Figure 4. 16Gate pulses for T5

For T4, T6 and T2, the gate signals are the inverse of T_1, T_3 and T_5 respectively. This is done by adding a NOT gate after each comparator and then the resultant signal is given to the remaining three switches in figure.4.17.Shown below.

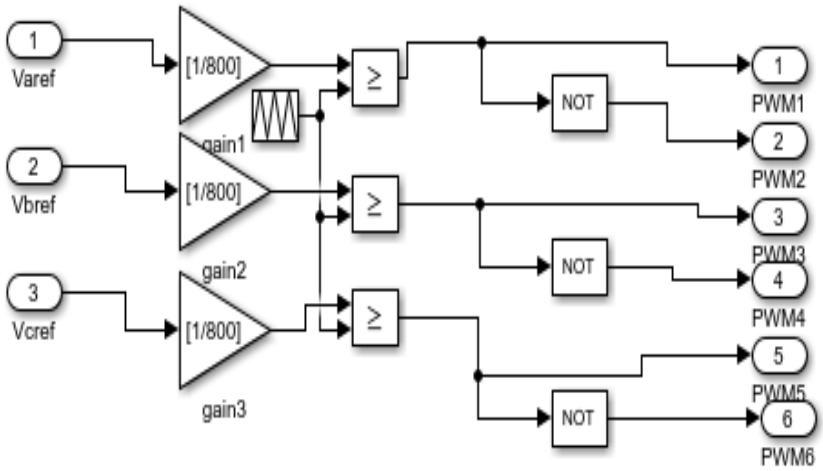

Figure 4. 17 Matlab schematic Sine pulse width modulation switching technique

To increase V_{ref} in order to control the amplitude of output voltage. The matlab simulation shows in figure.4.18.below in AC load have the same resistance value apply on the AC load. The resistor values are on the three AC load are R_1=500ohm, R_2=500ohm and R_3 =500ohm.Vref varies from 100v to 160v.

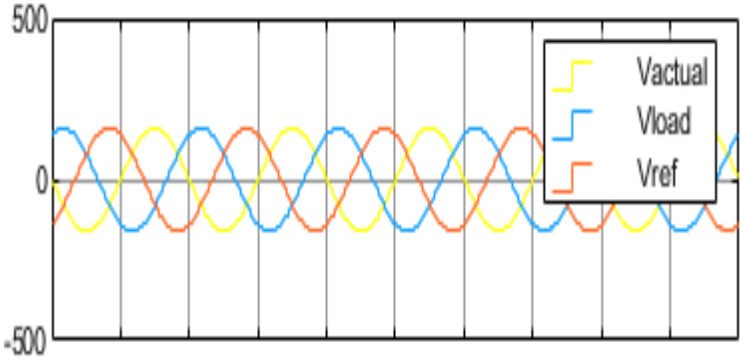

Figure 4. 18 Different reference voltage values.

In the figure.4.19.below the power flow from DC source to AC load first identify the AC load is excess means the higher inductive load happen for this case to sense the power factor is small. The DC load 80kw and AC load 200kw due to this the figure.4.19.a.the active power in AC bus shows 187kw.Figure .4.19.b. shows the reactive power value is very high due to inductive load values. Figure .4.19.c. shows the phase lag shift between current and voltage. Finally the power factor angle is around 82.5^0.

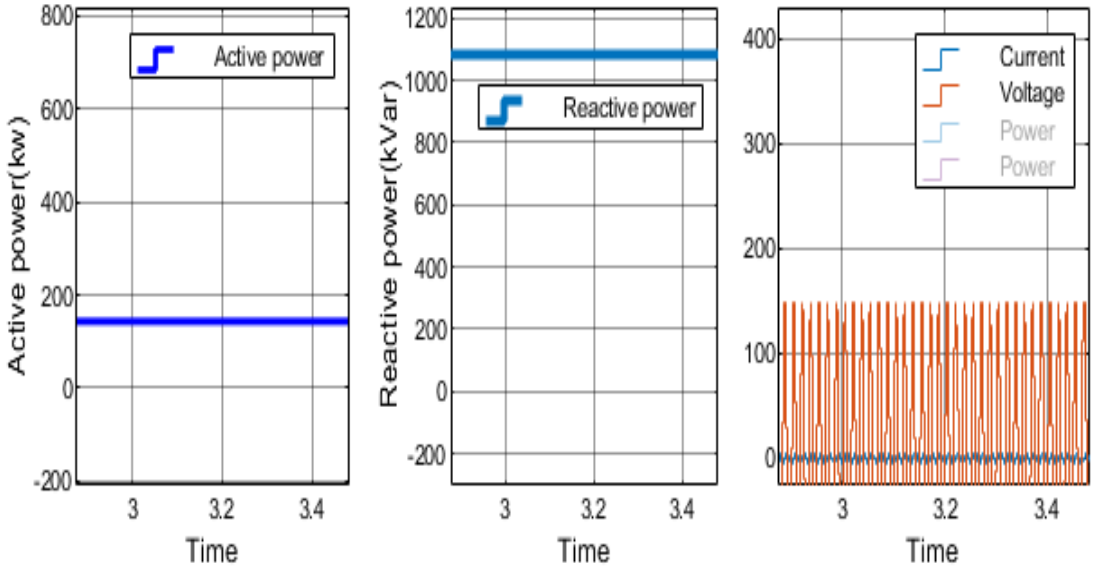

Figure 4. 19 AC load sensing

In figure .4.20.based the above load demands the FLC to limit the power load range.

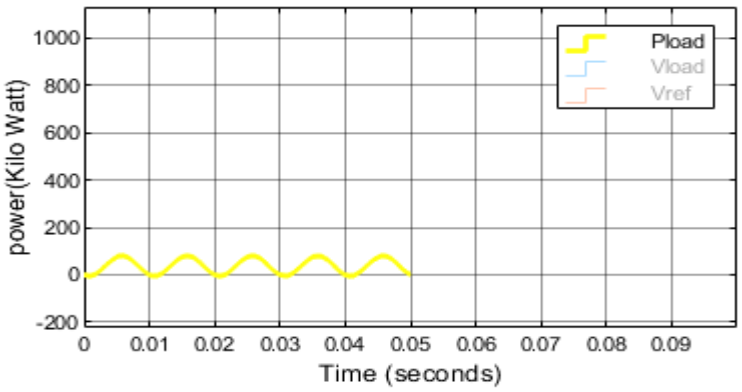

Figure 4. 20Power flow at the AC load.

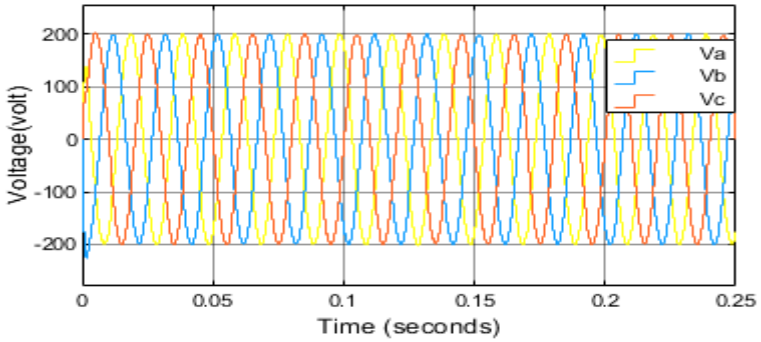

Figure 4. 21RMS line voltage

4.3.1 Matlab simulation of Inner Loop for AC Current Control dq reference

The control ways of the three phase inverter output current and voltage is formed by the control loops with higher speed and performance, and that act directly on the switches of the inverters. The aim of these controllers is to follow sinusoidal current and voltage references. A common implemented to perform the abc or dq transformation of the three-phase both currents and voltages in order to use two independent PI controller, one for each component.

The parameters used in the simulation are summarized in the following table.

Table 4. 3The parameters of simulation of inner loop AC current control

Parameter	Values
R_f	0.05 Ω
L_f	5mH
R_g	0.0073 Ω
L_g	0.76mH
w	100π rad/sec
i^*	25A(0-0.025s), 15A(0.025s)onward
Vref	400V

The variables frequency and voltage amplitude of the three phase AC side is to fix the operation, so a device is needed to regulate these variables. A bi-directional hybrid form of DC-AC three phase inverter is used for the active and reactive power dividing method to make stable the AC side in d-q coordinate. I_d is to controlled to regulated the active power passes through the three phase inverter to control the AC side frequency, whereas Iq is controlled to carry on the reactive power flow through the three phase Inverter to control the AC side voltages amplitude. The results of the inner loop simulation are given below based on the parameter given table 4.3.

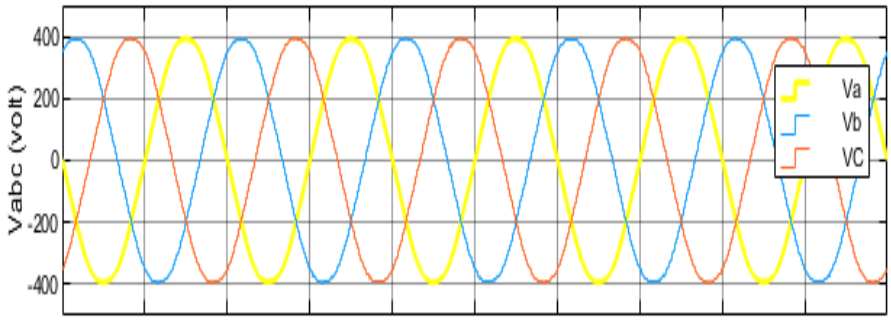

Figure 4. 22AC voltage

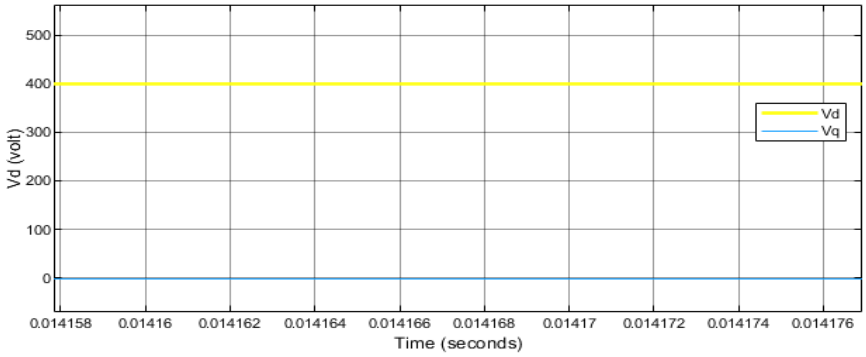

Figure 4. 23AC voltage dq reference.

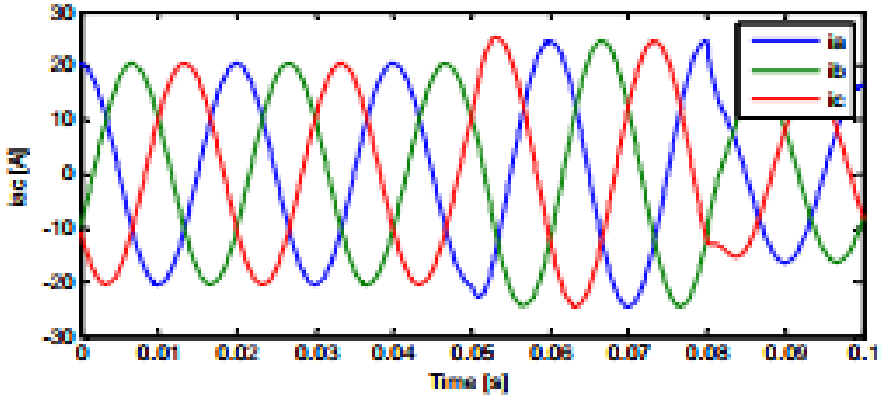

Figure 4. 24AC current

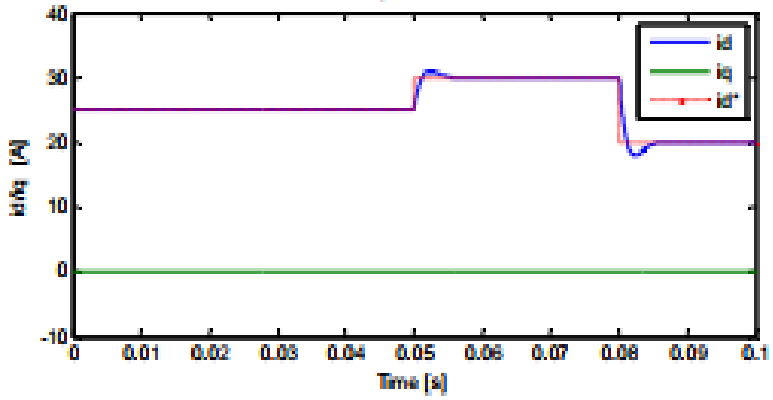

Figure 4. 25dq current

The DC source voltage is changed from 400v to 350v and the response of the overall system is enrolled. Change in the current provided by the source, changes the current injected into the AC side.

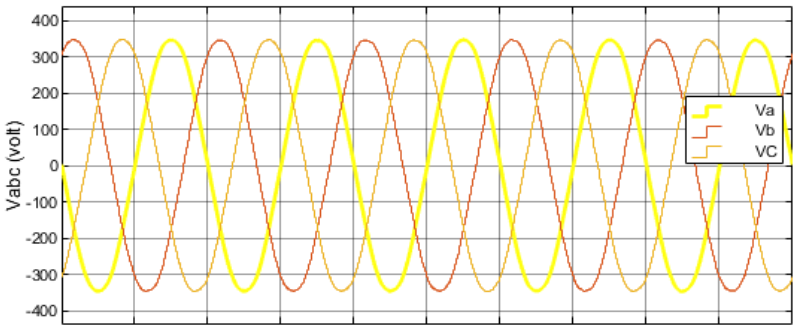

Figure 4. 26AC voltage

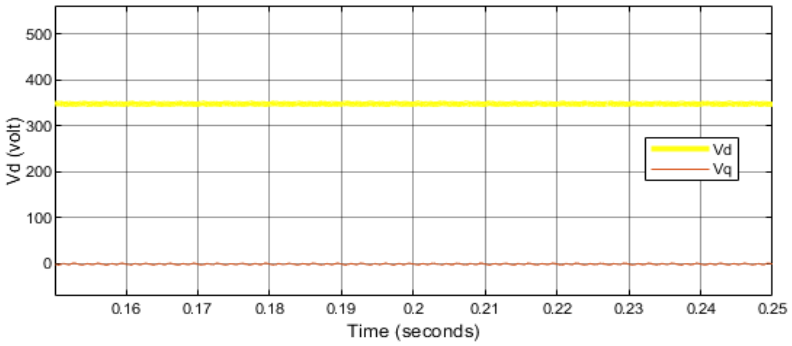

Figure 4. 27dq voltage

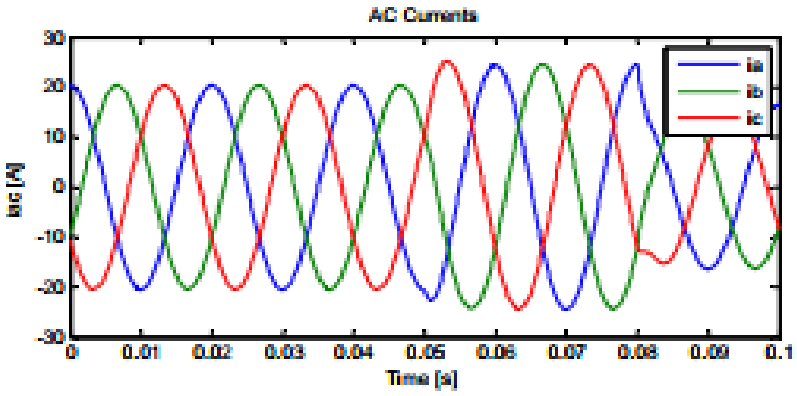

Figure 4. 28dq current control result

Case 3. DC load requires more power and operation act as converter AC to DC.

The Control methods for the three phase bi-directional converter AC to DC inverter is in in d-q cord mates, I_d is controlled to carry on the active power passes through the inverter to control the AC side frequency, and the same as I_q is controlled to carry on the reactive power passes through the Inverter to control the AC voltage amplitude. For this case I_q set to zero. The DC load require more power in the range 120kw-140kw and AC load in between 100kw to 120kw FLC generate the output 24kw to balance the load needed from AC supply.

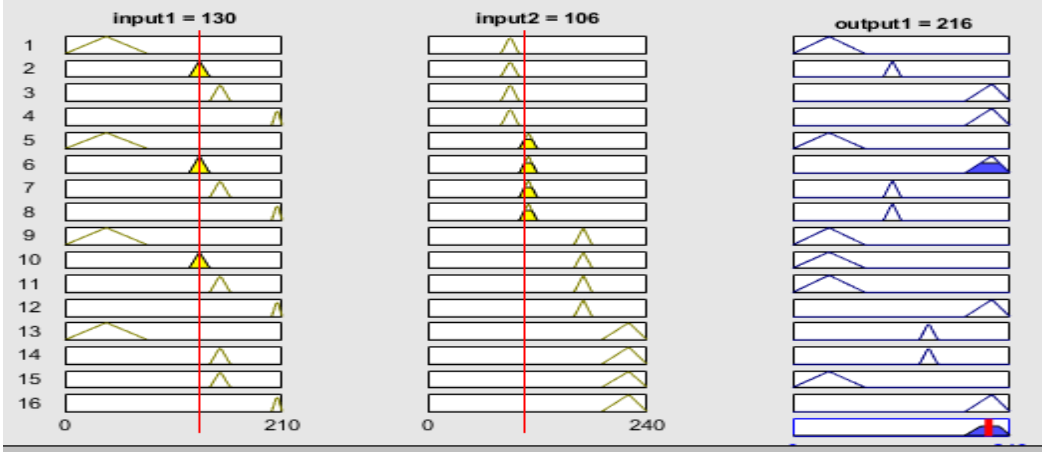

Figure 4. 29 Ruler view Generate DC-AC load demand by Fuzzy logic controller.

If the AC load is require more power in the range 100kw-120kw due to this DC load less then 80kw fuzzy logic controller generate the output 20kw load needed a power supply from DC source to AC load to balance the grid based on table.3.7.input-1 is DCload,input-2 AC load .

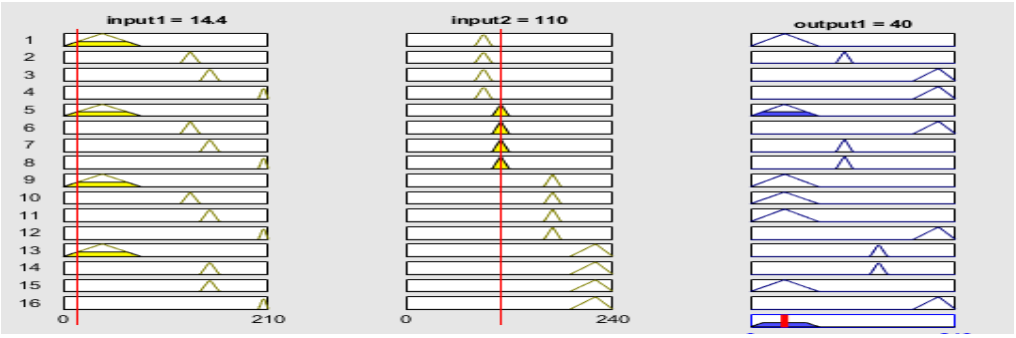

Figure 4. 30 Ruler view Generate DC-AC load demand by fuzzy logic controller

Once to identify the load demand, then active power pass from AC to DC is to alter the polarity after abc to dq reference of make V_d positive and I_d negative. The power flow through antiparallel diode the output power is 40kw at t=0.0684s and the load changes at t=0.0689s 23.56kw the power in the DC load based on figure 4.31.

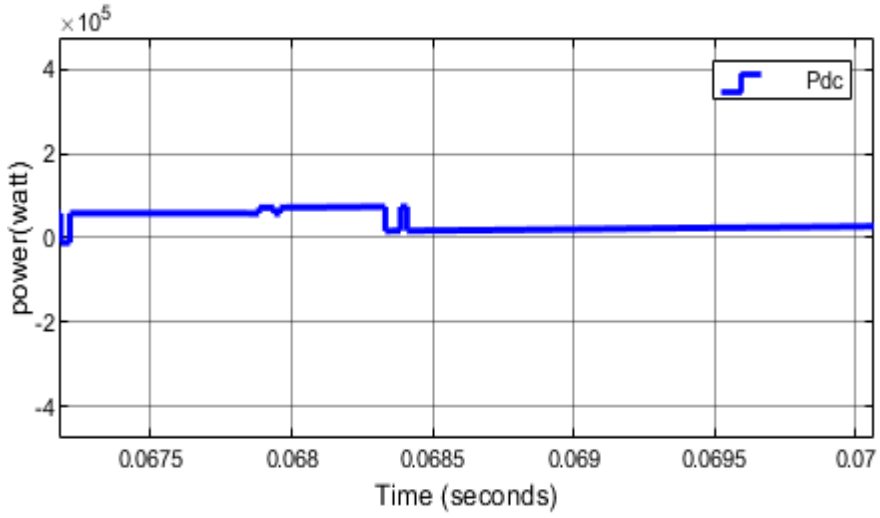

Figure 4. 31 Polarity change of Vd and Id the active power flow through the antiparallel diode.

4.4. Summary

In this chapter simulation results are discussed briefly. The dq0 transfer mapping of three-phase signal in the abc references frame into new variables in a rotating dq0 reference frame, controlled of active power and reactive power separately in dq reference frame. In DC micro grid the main components of are PV array, DC-DC boost converter, load and the MPPT control algorithm is simulations are implemented and the output power depends on the temperature and irradiation. The DC-DC boost converters for PV applications are the ability to supply a high voltage output from a low voltage input. The maximum power point tracking algorithm was implemented for pull out maximum functional power from PV module under a given environmental situations by controlling the duty ratio of DC-DC boost converter.

Also various load demand identify from AC bus and DC bus using fuzzy logic controller on voltage sensor in DC bus and in the AC bus to sense the power factor. The simulation for the three phase inverters is carried out in MATLAB/Simulink where a simple controlled method i.e. SPWM is applied for switching the switches gates, each of the transistors conducts for 180 degrees when AC load require more power. This SPWM technique is the method used to deliver gate signals to the other switches in three phase inverter operation mode. The total harmonic for different modulation index is obtained and compared for variable resistor load. When DC load require more power, then to change the polarity of V_d and I_d in dq reference, then the inverter act as rectifier power flow from AC bus to DC bus in the reverse diode.

CHAPTER-FIVE

5. CONCLUSION, RECOMANDATION AND FUTURE WORK

5.1. CONCLUSION

The modeling system of DC-AC micro-grid for power flow on both side of control system configuration is done in MATLAB/SIMULINK environment. The models are improved for the converters to affirm stable system under different loads; different resource conditions and the controls methods are studied. For best power tracking the maximum power point tracking (MPPT) algorithm is implemented to harness maximum power from PV DC sources and wind as AC source to coordinate the power exchange between DC and AC grid. This work also mainly included the interlinking converter (IC) in between AC micro-grid and DC micro-grid operation of hybrid. The controlled of the three phase VSC model in dq reference is the coupling between d and q axes and this model used to control of the inverter output of both voltage and current is formed by the control loops with higher speed and performance, and that act directly on the switches of the inverters. Therefore, the converter output impedance in this reference frame includes self and cross coupling impedances for two axes. A FLC identifies the load demand based on the design range using voltage sensor. If AC loads require more power means high inductive load with low power factor and the operation act as like inverter a simple controlled strategy SPWM is applied for switching the switches. If the DC load requires more power means to sense the current or voltage and the converter act as a rectifier mode i.e. to change the polarity of V_d and I_d. Although the hybrid DC-AC micro grid can minimized the processes of DC-AC and AC-DC conversions loss in a single AC or DC grid. The overall efficiency of the total system depends on the decrease of conversion losses and temperature and irradiation of PV for DC link and wind speed for AC link. Finally AC-DC interfacing can provide a reliable, high quality and more efficient power to the end consumer.

5.2. Recommendation

Renewable energy resources (Solar and Wind) in Ethiopia have in large abundant uses for electric power. So, I recommended that these resources to integrated in DC-AC micro grid and control the overall system using different intelligent controllers can improve the power efficiency of the system.

5.3. Future work

- The modeling, fault-tolerant control and control of fault diagnosis in DC-AC micro-grid voltage source converter using slide mode controller.
- The control mechanism can be develop for a micro-grid containing for large range of unbalanced and nonlinear loads using slide mode controller.

REFERENCES

[1] Parhizi, S.; Lotfi, H.; Khodaei, A.; Bahramirad, S. State of the art in research on micr grids: A review.IEEE Access 2015, 3,pp. 890–925. [CrossRef]

[2] Wang, X.; Guerrero, J.M.; Blaabjerg, F.; Chen, Z. Review of Power Electronics Based Micro grids. J. Power Electron. 2012, 12,pp.181–192. [CrossRef]

[3] Federal Democratic Republic of Ethiopia Ministry of Water and Energy "Scaling-up Renewable Energy program Ethiopia Investment Plan" January 2012 for Rural Village Electrification" Master Thesis.

[4] Lassetere RH, Paigi P (2004) Micro-grid: a conceptual solution. In: Proceedings of the 2004 IEEE power electronics specialists' conference, vol. 6, Aachen, Germany 20– 25 Jun 2004, pp.4285–4290.

[5] Swo CK, Lehn PW (2008) Control and power management of converter fed Micro Grids. IEEE Trans Power Syst 23(3),pp.1088–1098.

[6] Baran ME, Mahajan NR (2003) DC distribution for industrial systems: opportunities and challenges. IEEE Trans Ind Appl39(6),pp.1596–1601.

[7] Sannino A, Postiglione G, Bollen MHJ (2003) Feasibility of a DC network for commercial facilities. IEEE Trans Ind Appl39 (5):140.

[8] Mahmoodi M, Noroozian R, Gharehpetian GB et al (2007) A suitable power transfer control system for interconnection converter of DC micro grids. In: Proceedings of the 2007 international conference on renewable energies and power quality, vol.6, Sevilla 28–30 March 2007, pp. 2231–2237.

[9] Ito Z, Yang Z, Wkagi K (2004) DC micro grid based distribution power generation system. In: Proceedings of the 4th international power electronics and motion control conference (IPEMC), vol. 3, Xi'an China, 14–16 Aug 2004, pp. 1740–1745

[10] Wang P, Goel L, Liu X, Choo FH (2013) Harmonizing AC and DC: a hybrid AC/DC future grid solution. IEEE Power Energy Mag 11(3),pp.76–83.

[11] Kurohane K, Senjyu T, Yona A et al (2010) A hybrid smart AC/DC power system. IEEE Trans Smart Grid 1(2),pp.199–204.

[12] S. Peyghami, H. Mokhtari, and F. Blaabjerg, "Hierarchical Power Sharing Control in DC Micro grids," in Micro grid: Advanced Control Methods and Renewable Energy System Integration, First., Magdi S Mahmoud, Ed. Elsevier Science & Technology, 2017, pp. 63–100.

[13] J. Rocabert, A. Luna, F. Blaabjerg, and P. Rodriguez, "Control of Power Converters in AC Microgrids," IEEE Trans. Power Electron.,vol. 27, no. 11, pp. 4734–4749, 2012.

[14] S. Peyghami, H. Mokhtari, P. C. Loh, P. Davari, and F. Blaabjerg, Distributed Primary and Secondary Power Sharing in a Droop-Controlled LVDC Micro grid with Merged AC and DC Characteristics," IEEE Trans. Smart Grid, no. To be Published, DOI: 10.1109/TSG.2016.2609853, 2016.

[15] Jin J, Loh PC, Wang P, Mi Y, Blaabjerg F (2010) Autonomous operation of hybrid ac–dc micro grids. In: Proceedings 2010 IEEE international conference on sustainable energy technologies (ICSET), Kandy Sri Lanka, 6–9 Dec 2010, pp. 1–7

[16] Loh PC, Li D, Chai YK, Blaabjerg F (2013) Autonomous operation of hybrid micro grid with ac and dc sub grids.IEEE Trans Power Electron 28(5),pp.2214–2223.

[17] Loh PC, Blaabjerg F (2011) Autonomous control of distributed storages in micro grids. In: Proceedings of the IEEE 8th inter-national conference on power electronics and ECCE Asia, Jeju,South Korea, 30 May–3 Jun 2011, pp. 536–542.

[18] Loh PC, Li D, Chai YK et al (2013) Autonomous control of interlinking converter with energy storage in hybrid ac–dc micro grid. IEEE Trans Ind Appl 49(3),pp.1374–1382.

[19] Guerrero J, Vasquez J, Matas J, de Vicuna L, Castilla M. Hierarchical control of droop-controlled AC and DC micro grids – a general approach toward standardization. IEEE Trans Ind Electron 2011;58(1),pp.158–72.

[20] Morstyn T, Hredzak B, Agelidis V. Distributed cooperative control of micro grid storage. IEEE Trans Power Syst 2015;30(5),pp.2780–2795.

[21] Pogaku N, Prodanovic M,Green TC. Modeling, analysis and testing of autonomous operation of an inverter based micro grid. IEEE Trans Power Electron 2007;22(2), pp.613–625.http://dx.doi.org/10.1109/TPEL.2006.890003.

[22] Divshali PH, Alimardani A, Hosseinian SH, Abedi M. Decentralized cooperative control strategy of micro sources for stabilizing autonomous VSC based micro grids.IEEETrans Power Syst 2012;27(4), pp.1949–59.http://dx.doi.org/10.1109/TPWRS.2012.2188914.

[23] Hamidi RJ, Livani H, Hosseinian S, Gharehpetian G. Distributed cooperative control system for smart micro grids. Electr Power Syst Res 2016;130,pp.241–250.

[24] Loh PC, Blaabjerg F (2011) Autonomous control of distributed storages in micro grids. In: Proceedings of the IEEE 8th inter-national conference on power electronics and ECCE Asia, Jeju,South Korea, 30 May–3 Jun 2011, pp 536–542.

[25] Loh PC, Li D, Chai YK, Blaabjerg F (2013) Autonomous operation of hybrid micro grid with ac and dc sub grids. IEEE Trans Power Electron 28(5),pp.2214–2223.

[26] M. S. Ali, S. K. Kamarudin, M. S. Masdar, A. Mohamed. An Over all of Power Electronics Applications in Fuel Cell Systems : AC-DC Converters. Sci. World J. 2014; 2014,pp. 1–9.

[27] A. Narrekchi, S. L.ammoun, S. Sallem, M. B. A. Kammoun. A practical technique for connecting PV generator to single-phase grid. Sol. Energy. 2015; 118,pp.145–154.

[28] M. J. Ebrahimi, A. H. Viki. Interleaved Larg Step-up DC-DC Converter to a Diode Capacitor Multiplier and Ripple-Free Input Current. Bull. EEI. 2015; 4(4),pp. 289–297.

[29] W. Li, X. He. Review of Non isolated High-Step-Up DC/DC Converters in Photovoltaic Grid-connected Applications. IEEE Trans. Ind. Electron. Trans. 2011; 58 (4),pp. 1239–1250.

[30] S. J. Pinto, G. Panda. Wavelet methodes based on islanding detection and improved duplicative current control for reliable operation of grid-connected PV systems. Electr. Power Energy Syst. 2015;67,pp.39–51.

[31] O. Deveci, C. Kasnakoğlu. Performance improvement of a pv system of the model using a controller redesign based on numerical modeling. Int. J. Hydrogen Energy. 2016;41(29),pp. 12634–12649.

[32] M. H. Taghvaee, M. A. M. Radzi, S. M. Moosavain, H. Hizam, M. Hamiruce Marhaban. For current and the future study on non-isolated DC-DC converters for photovoltaic applications. Renew. Sustain. Energy Rev. 2013; 17,pp.216–227.

[33]. L. Fialho, R. Melıcio, V. M. F. Mendes, S. Viana, C. Rodrigues, A. Estanqueiro. A Simulation of hybrid PV conversion into electric grid. Sol. Energy, 2014; 110,pp. 578–594.

[34]. V. K. Kannan, N. Rengarajan. Investigating the performance of photovoltaic based DSTATCOM using I cosΦ algorithm. Int. J. Electr. Power Energy Syst. 2014; 54,pp. 376–386.

[35] V. K. Kannan,N. Rengarajan.Photovoltaic based distribution static compensator for power quality improvement. Int. J. Electr. Power Energy Syst. 2012; 42 (1),pp. 685692.

[36] J. J. Brey, C. R. Bordallo, J. M. Carrasco, E. Galván, A. Jimenez, E. Moreno. Power conditioning of fuel cell systems in portable applications. Int. J. Hydrogen Energy. 2007; 32,pp.1559–1566.

[37] L. Fialho, R. Melıcio, V. M. F. Mendes, S. Viana, C. Rodrigues, A. Estanqueiro. A simulation of hybrid pv conversion into electric grid. Sol. Energy, 2014;110,pp.578–594.

[38] L. Palma, M. H. Todorovic, P. Enjeti. Design Considerations for a Fuel Cell Powered DC-DC Converter for Portable Applications. in Twenty-First Annual IEEE Applied Power Electronics Conference and Exposition (APEC ’06). 2006,pp.1263-1268.

[39] Guerrero JM, Matas J, de Vicun ˜a LG et al (2006) Wireless-control strategy for parallel operation of distributed generation inverters. IEEE Trans Ind Electron 53(5),pp.1461–1470.

[40] S. M. Sharkh, M. A. Abusara, G. I. Orfanoudakis, and B. Hussain, Power Electronic

Converters for Microgrids. JohnWiley & Sons Singapore Pte. Ltd.,2014.

[41] J. Rocabert, A. Luna, F. Blaabjerg, and I. Paper, “Control of Power Converters in AC Microgrids,” IEEE Trans.E. Power Electron., vol. 27, no. 11, pp. 4734–4749, 2012.

[42] J. M. Guerrero, M. Chandorkar, T. Lee, and P. C. Loh, “Advanced Control Architectures for Intelligent Microgrids; Part I: Decentralize and Hierarchical Control stage,” Ind. Electron. IEEE Trans., vol. 60, no. 4, pp. 1254–1262, 2013.

[43] A. Egea-Alvarez, Multiterminal HVDC transmission systems for offshore wind, Barcelona,2014.

[44] K. Ogata, Ingeniería de Control Moderna, 4ª Edición, Madrid: Prentice-Hall, 2007.

[45] D. Jovčić and K. Ahmed, High-voltage direct-current transmission: converters, systems and dc grids, Wiley, 2015.

[46] Berihun G.(2013) modeling and simulating of a micro hydro wind double power generation system for rurals area of Ethiopia. Mater thesis in Addis Ababa University

[47] Golma Boyena, 2011 Design of a photovoltaic wind hybrid power generation system for Ethiopian remote area. Master thesis.

[48] Leak, E woldemaria “Genset solar wind hybrid power system of off-grid power generation forrural application.

[49] Getachew Bekele, Bjorn Palm, “Feasibility study for a standalone solar-wind-based hybrid energy system for application in Ethiopia”, Applied Energy, vol 87, pp487-495, 2010.

APPENDICES A

i). Matlab schematic representation Fuzzy logic controller design.

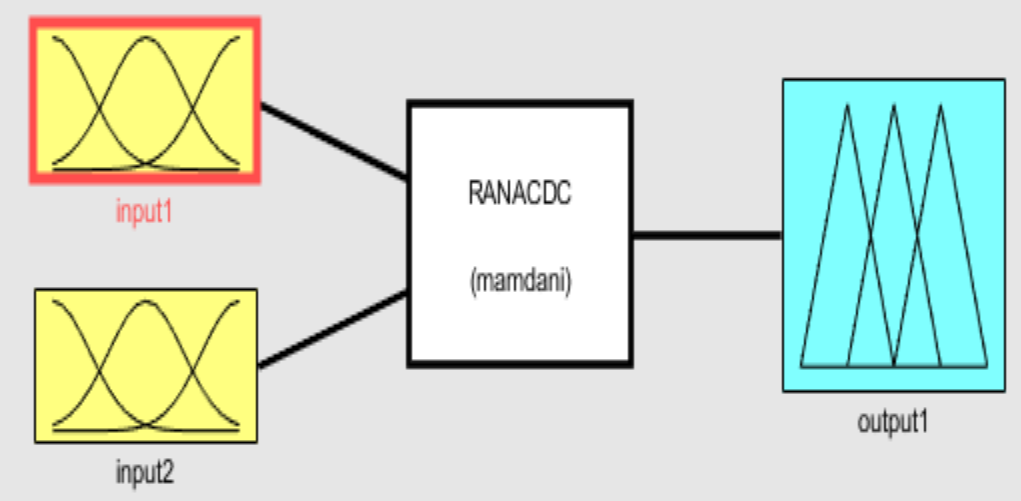

ii).Fuzzy logic controller membership function power load demand input 1.

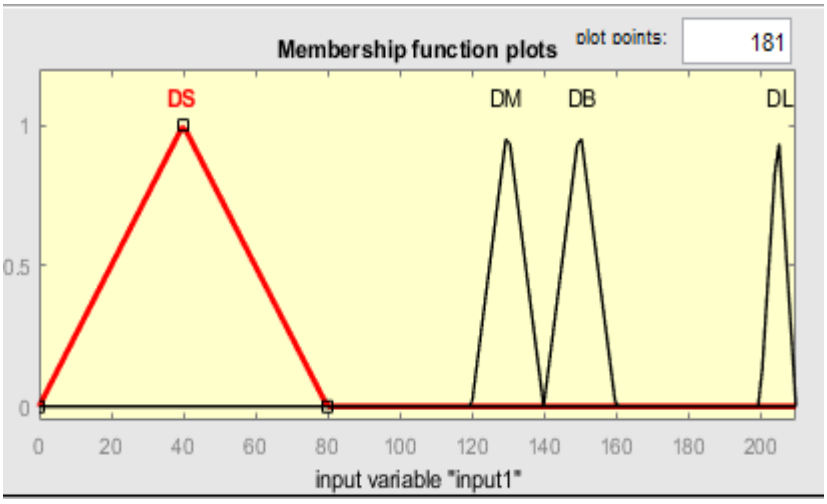

APPENDICES B

iii).Fuzzy logic controller membership function power load demand input 2.

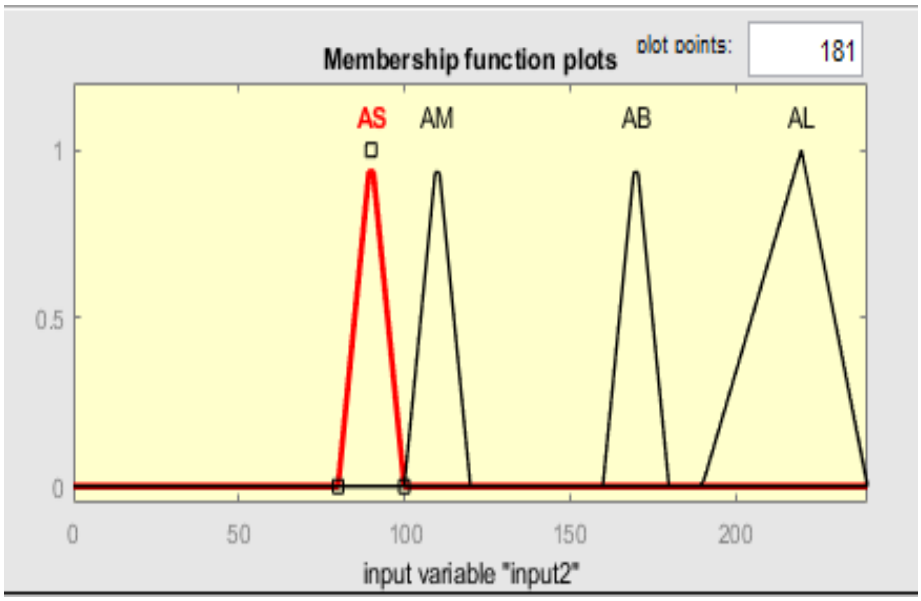

iv).Fuzzy logic controller membership functions of output load demand

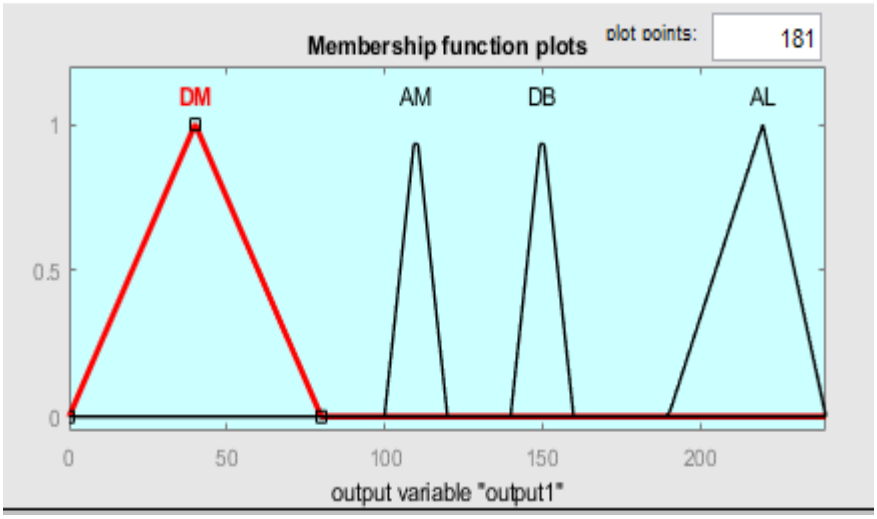

APPENDICES C

v) The inference mechanism engine uses the collection of 16 linguistic rules.

1. If (input1 is DS) and (input2 is AS) then (output1 is DM) (1)
2. If (input1 is DM) and (input2 is AS) then (output1 is AM) (1)
3. If (input1 is DB) and (input2 is AS) then (output1 is AL) (1)
4. If (input1 is DL) and (input2 is AS) then (output1 is AL) (1)
5. If (input1 is DS) and (input2 is AM) then (output1 is DM) (1)
6. If (input1 is DM) and (input2 is AM) then (output1 is AL) (1)
7. If (input1 is DB) and (input2 is AM) then (output1 is AM) (1)
8. If (input1 is DL) and (input2 is AM) then (output1 is AM) (1)
9. If (input1 is DS) and (input2 is AB) then (output1 is DM) (1)
10. If (input1 is DM) and (input2 is AB) then (output1 is DM) (1)
11. If (input1 is DB) and (input2 is AB) then (output1 is DM) (1)
12. If (input1 is DL) and (input2 is AB) then (output1 is AL) (1)
13. If (input1 is DS) and (input2 is AL) then (output1 is DB) (1)
14. If (input1 is DB) and (input2 is AL) then (output1 is DB) (1)
15. If (input1 is DB) and (input2 is AL) then (output1 is DM) (1)
16. If (input1 is DL) and (input2 is AL) then (output1 is AL) (1)

vi).Rule viewer fuzzy logic controller.

Input-1 power load range in kw (120-140), Input-2(100-120) and the output (190-240).

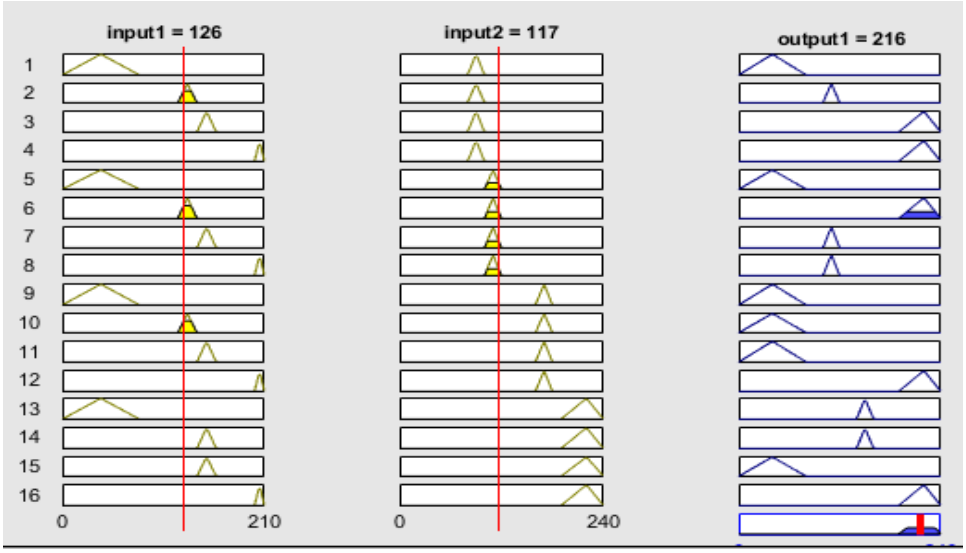

APPENDICES D

vii). Rule viewer fuzzy logic controller.

Input-1 power load rangein kw(140-160), input-2(100-120) and the output(100-120)

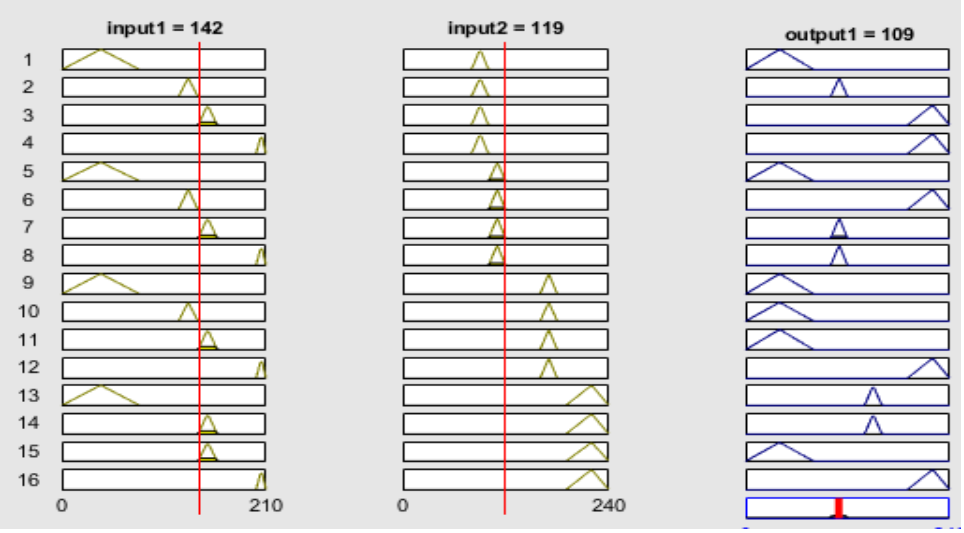

viii). Surface viewer of input-1,input-2 and output load range.

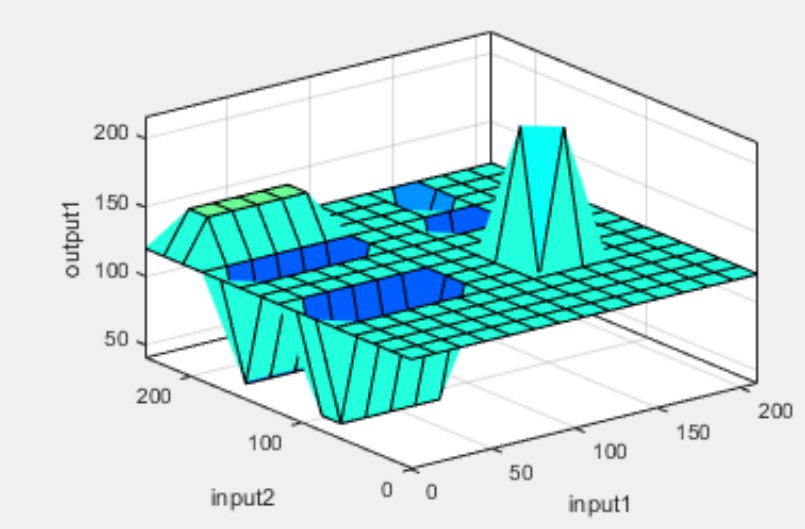

APPENDICES E

ix).Fuzzy logic controller modeling

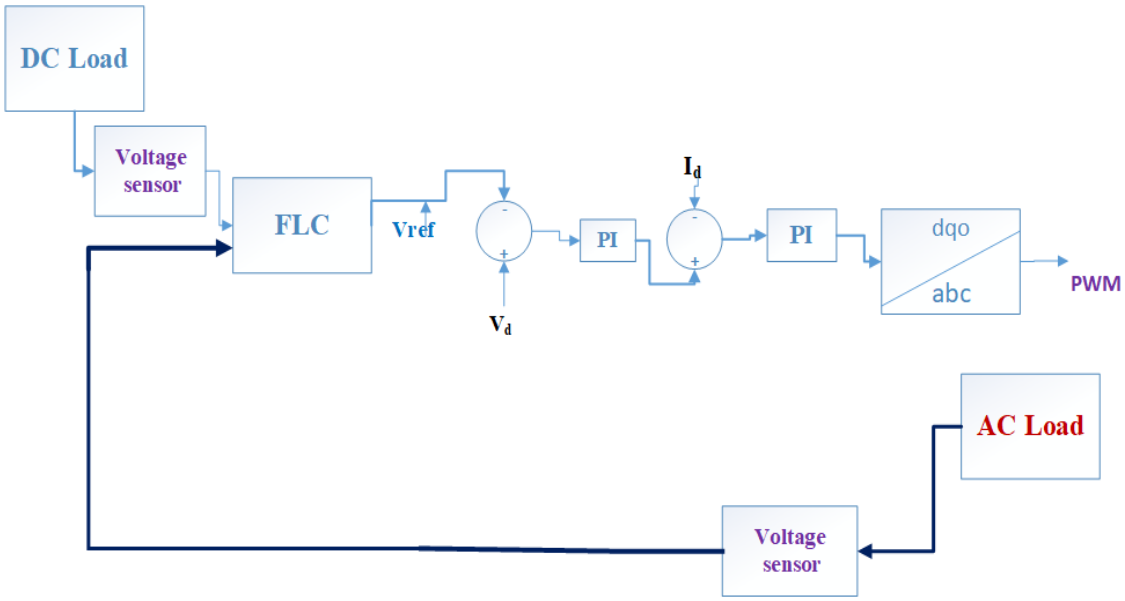

x).MPPT algorithm in matlab function.

Editor - Block: slx333/MATLAB Function1

MATLAB Function1

```
function D = MPPTPO(P,p,V,v,d)
dp=P-p;
dv=V-v;
d=0.54;


if(dp>0)
          if(dv<0)
             D=d+0.05;
           else
             D=d-0.05;

           end

else
           if(dv<0)
                D= d-0.05;
           else
               D= d+0.05;
```

APPENDICES F

xi).Matlab simulik model of AC load identify and measure the power factor.